

ProTeCt: Prompt Tuning for Hierarchical Consistency

Tz-Ying Wu* Chih-Hui Ho* Nuno Vasconcelos

Department of Electrical and Computer Engineering

University of California, San Diego

{tzw001, chh279, nvasconcelos}@ucsd.edu

Abstract

Large visual-language models, like CLIP, learn generalized representations and have shown promising zero-shot performance. Few-shot adaptation methods, based on prompt tuning, have also been shown to further improve performance on downstream datasets. However, these models are not hierarchically consistent. Frequently, they infer incorrect labels at coarser taxonomic class levels, even when the inference at the leaf level (original class labels) is correct. This is problematic, given their support for open set classification and, in particular, open-grained classification, where practitioners define label sets at various levels of granularity. To address this problem, we propose a prompt tuning technique to calibrate the hierarchical consistency of model predictions. A set of metrics of hierarchical consistency, the Hierarchical Consistent Accuracy (HCA) and the Mean Treecut Accuracy (MTA), are first proposed to benchmark model performance in the open-granularity setting. A prompt tuning technique, denoted as Prompt Tuning for Hierarchical Consistency (ProTeCt), is then proposed to calibrate classification across all possible label set granularities. Results show that ProTeCt can be combined with existing prompt tuning methods to significantly improve open-granularity classification performance without degradation of the original classification performance at the leaf level.

1 Introduction

Vision-language foundational models have opened up new possibilities for image classification. Traditionally, a classifier is designed by curating a dataset of labeled images and using it to train a deep network. This procedure has two main limitations, where the dataset must be sizeable and the label set must be fixed. Foundation models promise to eliminate these constraints. They are large models trained on huge training corpora of images and text and aim to learn a generic representation, where images and text are aligned. For example, Contrastive Language-Image Pretraining (CLIP) [33], combines text and image encoders trained with 400M image-text pairs in an open vocabulary fashion, using a contrastive loss [3, 4, 37, 38] based on positive and negative image-text pairs. Zero-shot classification can then proceed by using the alignment of image and text features. Each class name in the label set is first converted to a text prompt, e.g., “a photo of [CLASS],” which is fed to the text encoder. The resulting text feature is then used as the parameter vector of a softmax classifier of image feature vectors. Since the training does not emphasize any particular classes, CLIP supports an open vocabulary classification and its zero-shot performance is competitive with traditional classifiers fine-tuned on sizeable datasets. Its feature can also be transferred to various downstream tasks, including segmentation [41, 28] and 3D recognition [32, 47]. Several works [50, 49, 15, 45] have also shown that classification accuracy can be enhanced by fine-tuning the foundational model on the few-shot setting, i.e., with a few examples per class. To adapt the model and maintain the alignment between text and images, these works augment the foundational model with a few learnable prompts, either at the encoder input [50, 49, 45] or inside its transformer layers [15]. The model parameters are then frozen and only the prompts are optimized. This process is known as **prompt tuning** and can achieve significant improvement over the zero-shot performance, on the dataset of interest.

*Authors have equal contributions.

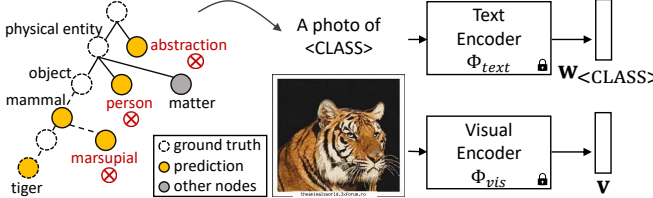


Figure 1: An example of class hierarchy, where CLIP predicts the tiger image as “person” at the internal hierarchy level.

While foundational models promise a shift to a much simpler world, where classifiers can be designed for virtually any classes with minimal dataset curation effort, the validity of this promise rests on the robustness of their image representation. One way to investigate this robustness is to require the classifier to perform hierarchical classification [51, 25, 44, 42, 19, 29], which requires it to understand the relations between the superclasses and subclasses that compose a class hierarchy, and provide correct predictions *across* hierarchy levels. Fig. 1 shows an example of a class hierarchy built from ImageNet [6] classes, according to the WordNet [10]. When faced with the image of a tiger, the classifier should provide a correct prediction under the label sets $\mathcal{Y}_1 = \{“dog”, “cat”, \textbf{“tiger”}\}$, $\mathcal{Y}_2 = \{“person”, “\textbf{animal}”, “insect”\}$ or $\mathcal{Y}_3 = \{“\textbf{physical entity}”, “abstraction”\}$, where the correct prediction is shown in bold. The failure to do so indicates two major problems. Theoretically, the model cannot really be called a foundational model. While it may understand class relations *locally*, e.g., perform well on a set of classes with a similar level of abstraction, it cannot support the *global* reasoning of human, e.g., the picture depicts a “tiger”, but not an “insect” nor an “abstraction”.

To study this problem, we introduce the notion of **hierarchical consistency**, and a new *hierarchical consistency accuracy* (HCA) metric, where classification is defined with respect to a taxonomic tree and its success requires the correct prediction of all superclasses (e.g., mammal, object and physical entity) of each ground truth leave class (e.g., tiger). This is complemented by the notion of classification with **open-granularity**, where classifiers can have any set of nodes in the class hierarchy as the label set, and a new *mean treecut accuracy* (MTA) metric, which estimates classification accuracy in this setting. Our experiments find that neither CLIP nor existing prompt tuning methods [50, 49, 15] performs well under HCA and MTA metrics. Fig. 1 illustrates the problem and the *inconsistent* CLIP class predictions (orange dots) across hierarchy levels. Table 1 compares the standard (leaf) accuracy of the model with HCA/MTA, under both the zero-shot and two prompt-tuning settings. While the leaf accuracy is quite reasonable, hierarchical consistency is very poor. To address this problem, we propose a novel prompt-tuning procedure, denoted *Prompt Tuning for Hierarchical Consistency* (ProTeCt) to improve the hierarchical consistency of existing prompting tuning. This is implemented by building a class hierarchy for the dataset of interest, whose classes are set as leaf nodes, and whose superclasses (internal nodes) are derived from the WordNet [10] taxonomy. Since foundation models support classification with open vocabulary, any node in the hierarchy can be used in the label set of the classifier. This is leveraged to introduce a regularization loss, the *dynamic treecut loss* (DTL), which encourages correct classification at all tree levels by sampling random tree cuts during training. This is complemented by a *node-centric loss* (NCL), which contributes additional supervision to each internal tree node and ensures classification robustness for all granularities of the hierarchy.

Experiments show that ProTeCt outperforms prior prompting tuning methods, CoOp [50] and MaPLe [15], under the HCA/MTA metrics by more than 15/25 points on Cifar100, SUN and ImageNet datasets. Following [50, 49, 15], we show that these gains hold for domain generalization experiments involving ImageNet variants [34, 39, 13, 12] under the zero-shot setting. ProTeCt again outperforms the vanilla CoOp and MaPLe, indicating that hierarchical consistency transfers across datasets. Furthermore, ablations show that ProTeCt can be used with different CLIP architectures and prompt tuning methods, further consolidating the effectiveness of the proposed contributions.

Overall, this work makes four contributions. First, we show that existing CLIP-type models do not fare well for hierarchical classification, by probing the prediction of CLIP-type models with respect to class hierarchies. Second, a novel prompt-tuning method, ProTeCt, is proposed to improve hierarchical consistency, by combining the DTL and NCL losses. The former relies on a dynamic stochastic sampling of label sets involving multiple levels of the hierarchy, while the latter regularizes the classification of every node in the hierarchy. Third, two novel evaluation metrics (HCA and MTA) for hierarchical classification are proposed. Finally, ProTeCt is shown to outperform vanilla prompt tuning methods on three datasets with different hierarchies. Extensive ablations demonstrate

Table 1: Evaluating hierarchical consistency in SOTA CLIP-based classifiers (w/ ViT-B/16).

Method	Acc_{leaf}	HCA	MTA
CLIP [33]	68.36	3.32	48.21
CoOp [50]	71.23	2.99	46.98
MaPLe [15]	70.70	4.15	48.29

that ProTeCt is applicable to different prompt tuning methods, CLIP architectures, and the learned hierarchical consistency transfers to unseen datasets from different image domains.

2 Preliminaries

CLIP. CLIP [33] is a foundational model composed of a text encoder Φ_{text} and a visual encoder Φ_{vis} , which extract features from text and images, respectively. The two encoders are optimized by contrastive training [38, 37, 4, 3] to create a joint representation for the two modalities. Since the encoders are learned from a large-scale corpus of image-text pairs, the features are general and support various downstream tasks, e.g., image classification [50, 49, 15, 45] and segmentation [41, 28].

Image Classification with CLIP. Given a label set $\mathcal{Y} = \{t_y\}_{y=1}^C$, a zero-shot classifier can be designed in the CLIP representation space by introducing a weight vector \mathbf{w}_y per class y . These weight vectors are obtained by simply using the class name t_y (e.g., “dog”) as a text encoder prompt, i.e., $\mathbf{w}_y = \Phi_{text}(Emb_t(t_y)) \in \mathbb{R}^k$, where $Emb_t(\cdot)$ is a word embedding. Given these weight vectors, an image classifier of label set \mathcal{Y} can be implemented by computing class posterior probabilities with

$$p(t_y | \mathbf{x}; \mathcal{Y}) = \frac{\exp(\cos(\mathbf{w}_y, \mathbf{v})/\tau)}{\sum_{t_j \in \mathcal{Y}} \exp(\cos(\mathbf{w}_j, \mathbf{v})/\tau)}, \quad (1)$$

where $p(t_y | \mathbf{x}; \mathcal{Y})$ is the probability of class label t_y given image \mathbf{x} , $\mathbf{v} = \Phi_{vis}(Emb_v(\mathbf{x})) \in \mathbb{R}^k$ the visual feature vector, $Emb_v(\cdot)$ an image embedding, $\cos(\cdot, \cdot)$ the cosine similarity metric, and τ a temperature hyperparameter. Classification performance can usually be improved by inferring the classifier parameters \mathbf{w}_y from multiple text prompts, e.g. by including context words such as a prompt prefix p = “a photo of”, or p = “a drawing of”, computing $\mathbf{w}_y = \Phi_{text}(Emb_t(\{p, t_y\}))$, and ensembling the vectors \mathbf{w}_y obtained from multiple prompts [33, 50]. This, however, requires multiple forward passes through Φ_{text} during inference and can be undesirable for downstream applications.

More efficient inference can be achieved with prompt tuning [50, 49, 15, 45], which leverages a set of learnable parameters $\{\mathbf{c}_m^t\}_{m=1}^M$ as context features. These are prepended to each class name embedding $Emb_t(t_y)$ as text prompts, to produce the weight vectors $\mathbf{w}_y = \Phi_{text}(\{\mathbf{c}_1^t, \dots, \mathbf{c}_M^t, Emb_t(t_y)\})$. Note that each \mathbf{c}_i^t has the same dimension as the word embedding. Given a training dataset $\mathcal{D} = \{(\mathbf{x}_i, y_i)\}_{i=1}^N$, context features can be end-to-end optimized with the cross-entropy loss

$$L_{\mathcal{Y}}(\mathbf{C}^t) = \frac{1}{N} \sum_{i=1}^N \sum_{t_j \in \mathcal{Y}} -\mathbb{1}(t_j = t_{y_i}) \log p(t_j | \mathbf{x}_i; \mathcal{Y}, \mathbf{C}^t) \quad (2)$$

for the classifier of (1), where $\mathbb{1}(\cdot)$ is the indicator function, and \mathbf{C}^t the matrix of context features. Similarly, learnable prompts \mathbf{c}_i^v can be inserted into the image branch, i.e. $\mathbf{v} = \Phi_{vis}(\{\mathbf{c}_1^v, \dots, \mathbf{c}_M^v, Emb_v(\mathbf{x})\})$, for better visual adaptation [14, 45, 15]. To prevent compromising the generalization of the CLIP embeddings, the parameters of the two encoders (i.e., Φ_{text}, Φ_{vis}) are frozen in the few-shot setting. In this paper, we consider two prompt tuning variants, CoOp [50] and MaPLe [15], the former using learnable prompts in the text branch, and the latter on both branches.

Class Taxonomy. A class taxonomy \mathcal{Y}^{tax} organizes classes into a graph where classes of similar semantics are recursively assembled into superclasses, at each graph node (e.g. “dog” is a superclass of “Chihuahua” and “Corgi”). For a tree hierarchy, \mathcal{T} , each node $n \in \mathcal{N}$ has a single parent and multiple child nodes $Chd(n)$, where \mathcal{N} is the set of tree nodes. Given a set of classes $\{t_y\}_{y=1}^C$, a tree hierarchy \mathcal{T} can be built by treating $\{t_y\}_{y=1}^C$ as leaf nodes (where $Chd(t_y) = \emptyset$), i.e., $Leaf(\mathcal{T}) = \{t_y\}_{y=1}^C$, and recursively grouping classes in a bottom-up manner until a single root node is created, according to the similarity relationships defined by the taxonomy \mathcal{Y}^{tax} . For example, ImageNet [6] classes can be organized into a tree with 1,000 leaf nodes using the WordNet [10] taxonomy. Nodes that are not at the leaves are denoted as internal nodes $\mathcal{N}^{int} = \mathcal{N} \setminus Leaf(\mathcal{T})$.

3 Probing Hierarchical Consistency in CLIP Predictions

Given a set of images $\{\mathbf{x}_i\}_{i=1}^N$ and corresponding labels $\{y_i\}_{i=1}^N$, where $y_i \in \{1, \dots, C\}$ and C the number of classes in a label set \mathcal{Y} , conventional training learns a feature extractor, usually a CNN or transformer, and a weight vector \mathbf{w}_y per class $y \in \mathcal{Y}$. While effective, this procedure has two strong limitations. First, it requires large dataset sizes N to produce good representations, which is difficult to achieve *low-shot classification*. Second, the feature representation is optimal only for the *fixed set* of C classes in \mathcal{Y} . Its transfer to a new problem involving different classes usually

requires finetuning on a new dataset. While this requires a smaller dataset than that initially used to pre-train the model, its size N must still be substantial. The introduction of foundation models, like CLIP, promises to change this since 1) the weight vectors can be *inferred* from the text encoder and, 2) the feature representation is learned from a very large dataset, without emphasis on any particular classes. Several works have shown that few-shot training is possible with simple network adaptations [50, 49, 45] for several common datasets [6, 18, 43, 21, 30, 17]. Since the foundation model is trained with open vocabulary, it becomes possible to perform classification for any set of C classes, i.e., the representation supports *open-set* classification.

For practitioners, the foundation model paradigm promises a shift to a much simpler computer vision world, where classifiers can be trained for virtually any classes with very limited effort in dataset collection. However, this promise rests on the robustness of the foundation model representation. One problem is that, under the open-set setting, practitioners are free to define classification problems at many levels of class granularity, or even mix classes of different granularity. We refer to this as *open-granularity* classification. Even if the foundational model is tuned to a particular label set \mathcal{Y} , it should still support classification with respect to superclasses of the classes in \mathcal{Y} , e.g. “dog” vs. “cat” instead of “Chihuahua” vs. “Siamese”. This places on the representation the requirement to encode taxonomic constraints. In fact, it can be claimed that any representation which fails to encode these constraints is not really a foundational representation, neither does it really support open-set classification. After all, any human child knows that a “dog” is an “animal” and most people know that a “Chihuahua” is a “dog.” It is, however, not clear that this hierarchical consistency holds for CLIP, e.g., that it will always classify “Chihuahua” images as images of the “dog” class as well.

To test this, we performed an experiment where we implemented the classification rule

$$\hat{y}(\mathbf{x}; \mathcal{Y}) = \arg \max_{t_y \in \mathcal{Y}} p(t_y | \mathbf{x}; \mathcal{Y}). \quad (3)$$

for label sets \mathcal{Y} of different granularity, according to the ImageNet taxonomy. Using the ImageNet-1k [6] dataset, we defined the set of ImageNet classes as the leaf label set \mathcal{Y}_{leaf} and built the class hierarchy \mathcal{T} , denoting by $\mathcal{Y}_n = Chd(n)$ the set of class labels for the children of node n . We then compared the **Leaf Accuracy**,

$$Acc_{leaf} = \frac{1}{N} \sum_{i=1}^N \mathbb{1}[\hat{y}(\mathbf{x}_i; \mathcal{Y}_{leaf}) = t_{y_i}] \quad (4)$$

to the **Hierarchical Consistent Accuracy (HCA)**,

$$HCA = \frac{1}{N} \sum_{i=1}^N \left(\mathbb{1}[\hat{y}(\mathbf{x}_i; \mathcal{Y}_{leaf}) = t_{y_i}] \prod_{n \in \mathcal{A}(t_{y_i})} \mathbb{1}[\hat{y}(\mathbf{x}_i; \mathcal{Y}_n) \in \mathcal{A}(t_{y_i}) \cup \{t_{y_i}\}] \right), \quad (5)$$

where $\mathcal{A}(n)$ denotes all the ancestors of node n , and t_{y_i} is the leaf node corresponding to class label y_i . While Acc_{leaf} considers successful any correct classification at the leaf level of the tree, the *HCA* is stricter. It declares a success only when all the ancestors of the leaf node are correctly classified. In other words, each sample needs to be classified correctly at each tree level to be viewed as correctly classified by *HCA* computation. Acc_{leaf} is an upper bound for *HCA*. To estimate the expected accuracy under the open-granularity classification setting, we also measured the **Mean Treecut Accuracy (MTA)** metric. This measures the average accuracy over a set of treecuts $\mathcal{T}_c \in \Omega$ randomly sampled from \mathcal{T} ,

$$MTA = \frac{1}{|\Omega|} \sum_{\mathcal{T}_c \in \Omega} \frac{1}{N} \sum_{i=1}^N \mathbb{1}[\hat{y}(\mathbf{x}_i; \mathcal{Y}_{\mathcal{T}_c}) = t_{y_i}], \quad (6)$$

where $\mathcal{Y}_{\mathcal{T}_c} = Leaf(\mathcal{T}_c)$. Table 1 shows the performance of CLIP and prompt tuning methods under these three metrics. It is clear that *HCA* drops significantly from Acc_{leaf} for all methods, i.e. none of them maintains correct predictions within the class hierarchy and that the expected accuracy under the open-granularity setting is much smaller than that of classification with the leaf classes.

4 ProTeCt: Prompt Tuning for Hierarchical Consistency

To enhance the hierarchical consistency of the predictions at different hierarchical levels, we propose to regularize the model by *Prompt Tuning for Hierarchical Consistency* (ProTeCt). ProTeCt can

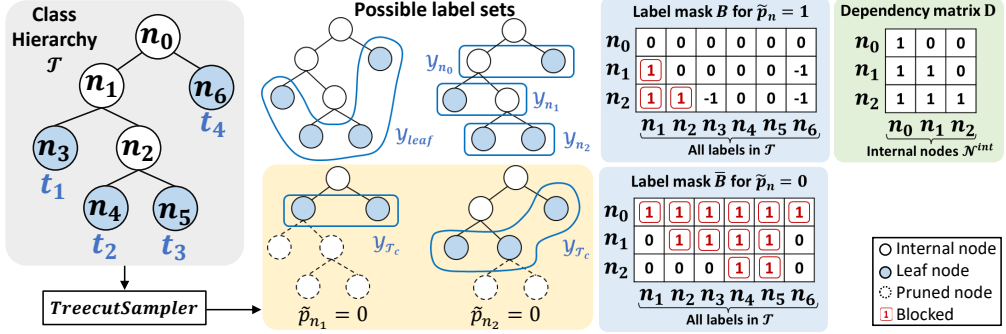


Figure 2: (Left) Multiple possible label sets are available in a class hierarchy. (Right) Predefined matrices for efficient treecut sampling, used in Algorithm 1.

be easily implemented with many existing prompt tuning methods (e.g., CoOp, MaPLE). These methods optimize context prompts using the cross-entropy loss of (2) with leaf label set \mathcal{Y}_{leaf} . While this optimizes leaf accuracy Acc_{leaf} , it is not robust to label set changes, even for label sets comprised of superclasses of \mathcal{Y}_{leaf} . A simple generalization would be to replace (2) with $\mathcal{L}(\mathbf{C}^t) = \sum_{\mathcal{Y}_p \in \mathcal{T}} L_{\mathcal{Y}_p}(\mathbf{C}^t)$, i.e., to consider all the partial label sets \mathcal{Y}_p of the tree \mathcal{T} . However, for sizeable taxonomies, this involves a very large number of label sets and is not feasible. ProTeCt avoids the problem by dynamically sampling label sets from \mathcal{T} during training, with a combination of two learning objectives, a *node-centric loss* (NCL) and a *dynamic tree-cut loss* (DTL).

Node-Centric Loss (NCL). NCL is the aggregate cross-entropy loss of (2) over all node-centric label sets $\mathcal{Y}_n = Chd(n)$ defined by each internal node $n \in \mathcal{N}^{int}$ of the hierarchy, i.e.,

$$\mathcal{L}_{NCL}(\mathbf{C}^t) = \frac{1}{|\mathcal{N}^{int}|} \sum_{n \in \mathcal{N}^{int}} L_{\mathcal{Y}_n}(\mathbf{C}^t). \quad (7)$$

NCL optimization encourages prompts that robustify the classification at the different granularities. For example, “Corgi” should be classified as “mammal” within the animal label set $\mathcal{Y}_{n_1} = \{\text{mammal, reptile, bird}\}$, as a “dog” within the mammal label set $\mathcal{Y}_{n_2} = \{\text{dog, cat, elephant, tiger}\}$, and so forth.

Dynamic Treecut Loss (DTL). While NCL calibrates node classification, guaranteeing consistency within each node, the label sets of open-granularity classification can also span different sub-trees of the hierarchy, including nodes at different levels, e.g., $\mathcal{Y} = \{\text{dog, cat, elephant, tiger, reptile, bird}\}$. DTL seeks to calibrate such label sets, by aggregating the cross-entropy loss of (2) dynamically, i.e., on an example basis, over randomly sampled label sets $\mathcal{Y}_{\mathcal{T}_c} = Leaf(\mathcal{T}_c)$ comprised of the leaves of the tree cuts \mathcal{T}_c (sub-trees) of \mathcal{T} . At each training iteration, a random tree cut \mathcal{T}_c is sampled with the *TreeCutSampler* procedure of Algorithm 1, as illustrated on the middle of Fig. 2, to define the loss

$$\mathcal{L}_{DTL}(\mathbf{C}^t) = L_{\mathcal{Y}_{\mathcal{T}_c}}(\mathbf{C}^t) \quad \mathcal{T}_c \sim TreeCutSampler(\mathcal{T}, \beta), \quad (8)$$

where $\beta \in [0, 1]$ is a rate of tree dropout. For this, a Bernoulli random variable $P_n \sim Bernoulli(\beta)$ of dropout rate β is defined for each internal node $n \in \mathcal{N}^{int} \setminus n_0$. The algorithm descends the tree \mathcal{T} , sampling a binary drop-out variable p_n at each node. If $p_n = 1$, node n is kept in the pruned tree \mathcal{T}_c . Otherwise, the sub-tree of \mathcal{T} rooted with n is dropped from \mathcal{T}_c . The parameter β controls the degree of pruning. Larger β induces the pruning of more tree nodes, while $\beta = 0$ guarantees that $\mathcal{Y}_{\mathcal{T}_c} = \mathcal{Y}_{leaf}$. The root node n_0 is excluded, as $p_{n_0} = 0$ would imply discarding the whole \mathcal{T} .

The *TreeCutSampler* algorithm is an efficient procedure to sample tree cuts \mathcal{T}_c from \mathcal{T} . It starts by sampling a vector $\mathbf{p} = (p_{n_1^{int}}, \dots, p_{n_K^{int}})$, where n_i^{int} denotes the i -th internal node and $K = |\mathcal{N}^{int}|$, containing pruning flags p_n for all internal nodes $n \in \mathcal{N}^{int}$. The next step is to enforce consistency between these flags, according to the tree structure. If any node in $\mathcal{A}(n)$ is pruned, then node n should be pruned even if $p_n = 1$. This is efficiently enforced across all the flags by defining a dependency matrix $\mathbf{D} \in \{0, 1\}^{K \times K}$ where $\mathbf{D}_{ij} = \mathbb{1}[n_j^{int} \in \mathcal{A}(n_i^{int}) \cup \{n_i^{int}\}]$ indicates whether the i -th internal node n_i^{int} depends on the j -th internal node n_j^{int} . An example is provided on the right of Fig. 2 for the tree on the left. The sampled flags are then corrected by computing $\tilde{\mathbf{p}} = \mathbf{p} \otimes \mathbb{1}[\mathbf{D}\mathbf{p} = \mathbf{D}\mathbf{1}]$, where $\mathbf{1}$ is the vector of K ones and \otimes the Hadamard product. Note that both \mathbf{D} and $\mathbf{D}\mathbf{1}$ are pre-computed, making the complexity of this step roughly that of one matrix-vector multiplication.

Algorithm 1 Treecut Sampler

Input: The tree hierarchy \mathcal{T} of the dataset, tree dropout rate β
Output: The treecut label set $\mathcal{Y}_{\mathcal{T}_c}$

```

// sampling p for internal nodes; prune the sub-tree rooted at n if  $p_n = 0$ 
 $p_{n_0} \leftarrow 1$ ; // always keep the root node
for  $n \in \mathcal{N}^{int} \setminus n_0$  do
     $p_n \leftarrow Bernoulli(\beta)$ 
 $p \leftarrow (p_{n_1^{int}}, \dots, p_{n_K^{int}})$ 
// correct p based on the dependency between internal nodes
 $\tilde{p} \leftarrow p \otimes \mathbb{1}[Dp = D1]$ 
// obtain blocked labels with predefined masks and the sampled  $\tilde{p}$ 
 $b \leftarrow \min(B, 0)^T \tilde{p} + \bar{B}^T(1 - \tilde{p})$ 
// gather available (unblocked) labels as the sampled label set
 $\mathcal{Y}_{\mathcal{T}_c} \leftarrow \{n_j : n_j \in \mathcal{N} \setminus n_0, b_j = 0\}$ 
return  $\mathcal{Y}_{\mathcal{T}_c}$ 

```

To identify the leaves of the sampled treecut ($\mathcal{Y}_{\mathcal{T}_c} = Leaf(\mathcal{T}_c)$) efficiently, a mask $B \in \{0, 1, -1\}^{K \times |\mathcal{N} \setminus \{n_0\}|}$ is defined, where each row corresponds to an internal node, and the columns contain all possible labels in \mathcal{T} , i.e., all nodes except the root n_0 . Entry B_{ij} flags that n_j cannot appear in the sampled label set, given that $n_i \in \mathcal{N}^{int}$ has not been pruned (i.e., $\tilde{p}_{n_i^{int}} = 1$), as follows

$$B_{ij} = \begin{cases} 1, & \text{if } n_j \in \mathcal{A}(n_i^{int}) \cup \{n_i^{int}\} \quad (n_j \text{ is an ancestor of } n_i^{int}) \\ 0, & \text{if } n_i^{int} \in \mathcal{A}(n_j) \quad (n_j \text{ is a descendant of } n_i^{int}) \\ -1, & \text{otherwise} \quad (n_j \text{ is outside of the sub-tree rooted at } n_i^{int}) \end{cases}. \quad (9)$$

Similarly, a matrix \bar{B} , of entries $\bar{B}_{ij} = 1 - |B_{ij}|$, is defined to flag that n_j cannot appear in the label set, given that $n_i \in \mathcal{N}^{int}$ has been pruned, i.e. $\tilde{p}_{n_i^{int}} = 0$. A mask of the nodes unavailable to the label set is then computed by accumulating the masks corresponding to the values of \tilde{p} ,

$$b = \min(B, 0)^T \tilde{p} + \bar{B}^T(1 - \tilde{p}), \quad (10)$$

where the mask in $\min(B, 0)$ is selected if $\tilde{p}_n = 1$, and that in \bar{B} if $\tilde{p}_n = 0$. Note that $\min(B, 0)$ clips $B_{ij} = -1$ to 0. The mask b can then be used to obtain $\mathcal{Y}_{\mathcal{T}_c} = Leaf(\mathcal{T}_c) = \{n_j : n_j \in \mathcal{N} \setminus n_0, b_j = 0\}$. Fig. 2 gives an example. When $\tilde{p} = (\tilde{p}_{n_0}, \tilde{p}_{n_1}, \tilde{p}_{n_2}) = (1, 0, 0)$, then $b = \min(B_1, 0) + \bar{B}_2 + \bar{B}_3 = (0, 1, 1, 2, 2, 0)$, signaling that only n_1 and n_6 are available to the label set (as $b_1, b_6 = 0$), resulting in $\mathcal{Y}_{\mathcal{T}_c} = \{n_1, n_6\}$. More detailed examples are given in the appendix.

Optimization. The overall loss used for prompt tuning is a combination of the two losses

$$\mathcal{L}(\mathbf{C}^t) = \mathcal{L}_{DTL}(\mathbf{C}^t) + \lambda * \mathcal{L}_{NCL}(\mathbf{C}^t) \quad (11)$$

where λ is a hyperparameter. Note that, like previous prompting approaches, ProTeCt optimizes the learnable prompts $\{\mathbf{c}_m\}_{m=1}^M$ while keeping the parameters of Φ_{text}, Φ_{vis} frozen.

5 Experiments

In this section, we discuss experiments for evaluating the effectiveness of ProTeCt. To demonstrate that ProTeCt is a plug-an-play method, it was applied to two SOTA prompt tuning methods: CoOp [50] and MaPLe [15]. Each experiment is averaged over 3 runs and full tables with error bars are shown in the appendix for brevity. All experiments were conducted on a single Nvidia A10 GPU, using Pytorch [31]. Please see the appendix for more training details and results. ProTeCt code builds on the publicly available codebases for CoOp and MaPLe and will be released upon publication.

Datasets: Three datasets are used for training ProTeCt prompts: Cifar100 [18], SUN [43] and ImageNet [6]. In all cases, we use the dataset classes as leaf nodes and build a taxonomy using WordNet [10]. The resulting class hierarchies are as follows. Cifar100 [18] contains 100 leaf nodes and 48 internal nodes. SUN contains 324 leaf nodes and 19 internal nodes (after pruning 73 leaf classes that have confusing superclasses). ImageNet [6], ImageNetv2 [34] and ImageNet-S [39] share a class hierarchy of 1,000 leaf nodes and 368 internal nodes. ImageNet-A [13] and ImageNet-R [12] only contain 200 subclasses and the corresponding internal nodes from the ImageNet hierarchy. For each dataset, the K-shot setting is considered, where K images per class are sampled for training.

Table 2: Prompt tuning performance with/without ProTeCt on Cifar100 ($\lambda = 0.5$), SUN ($\lambda = 0.5$) and ImageNet ($\lambda = 1$) dataset. $\beta = 0.1$ for all datasets.

Method	K-Shot	w/ ProTeCt	Cifar100			SUN			ImageNet		
			Acc _{leaf}	HCA	MTA	Acc _{leaf}	HCA	MTA	Acc _{leaf}	HCA	MTA
CoOp	16		72.88	10.04	50.64	73.82	38.28	52.99	71.23	2.99	46.98
	16	✓	72.94	56.85	87.69	74.59	62.94	83.51	69.92	37.74	88.61
	(+0.06)	(+46.81)	(+37.05)	(+0.77)	(+24.66)	(+30.52)	(-1.31)	(+34.75)	(+41.63)		
	1		65.03	7.81	41.78	63.65	33.36	51.20	63.67	1.59	40.52
MaPLe	16		75.01	17.54	52.21	71.86	33.25	54.29	70.70	4.15	48.29
	16	✓	75.34	61.15	88.33	72.17	59.71	82.27	69.52	31.24	87.87
	(+0.33)	(+43.61)	(+36.12)	(+0.31)	(+26.46)	(+27.98)	(-1.18)	(+27.09)	(+39.58)		
	1		68.75	4.65	50.60	63.98	25.15	50.31	68.91	2.97	48.16
	1	✓	69.33	48.10	83.78	64.29	50.45	76.73	66.16	20.44	85.18
	(+0.58)	(+43.45)	(+33.18)	(+0.31)	(+25.30)	(+26.42)	(-2.75)	(+17.47)	(+37.02)		

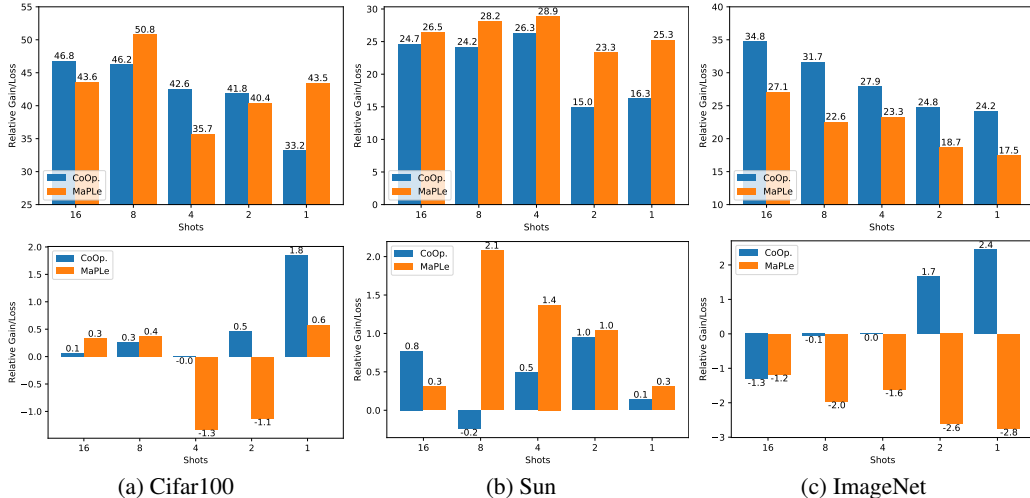


Figure 3: Relative gain/loss after adding ProTeCt under HCA (Top row) and Acc_{leaf} (Bottom row).

Metrics: Acc_{leaf} of (4), HCA of (5) and MTA of (6) are considered. MTA uses 5 tree dropout rates ($\beta \in \{0.1, 0.3, 0.5, 0.7, 0.9\}$) to sample treecuts of various granularities. For each β , T treecuts are sampled without repetition, to obtain a total of $5T$ treecuts. MTA is averaged over these $5T$ treecuts. We use $T = 5$ for all datasets.

Training Details: All vanilla prompt tuning and their ProTeCt counterparts are trained under the same setting. The following configuration is used unless noted. All experiments use SGD optimizer and the learning rate is set to 0.02 with a cosine learning rate scheduler. By default, a pretrained ViT-B/16 CLIP model is used as initialization. For Cifar100 and SUN, we train both CoOp and MaPLe prompts for 200 epochs, using a batch size of 128 and 32, respectively. For ImageNet, CoOp is trained for 30 epochs with a batch size of 8, while MaPLe is trained for 10 epochs with a batch size of 2. Note that the setting is slightly different from the original paper due to our GPU availability.

5.1 Improved Hierarchical Consistency with ProTeCt

Table 2 shows that vanilla CoOp and MaPLe have reasonable leaf accuracy for both 1-shot and 16-shot classification on Cifar100, SUN, and ImageNet. However, their very low HCA shows that their predictions are not consistent over the class hierarchy. In result, their classification performance in the open-granularity setting (MTA) is much weaker than their leaf accuracy. For example, 16-shot classification with CoOp on ImageNet has a leaf accuracy of 71.23, but expected open-granularity accuracy of 46.98. This is explained by the very low HCA of 2.99. Similar observations hold for different few-shot configurations. In all cases, ProTeCt (results on rows with a checkmark) significantly improves HCA and MTA. For example, it boosts the HCA of 16-shot classification with CoOp on ImageNet by 34.75 (2.99 vs 37.74), leading to an increase of MTA of 41.63 (46.98 to 88.61). Note that, in all cases, the MTA after ProTeCt training is *higher* than the leaf accuracy. This is expected for a well calibrated classifier, since decisions at intermediate levels of the tree are coarser-grained than those at the leaves, which can easily require very fine class distinctions.

Table 3: The gain of hierarchical consistency after adding ProTeCt generalizes across datasets in unseen domains. All methods are fine-tuned on ImageNet and evaluated on its 4 variants.

Method	K-Shot	w/ ProTeCt	ImageNetv2 [34]			ImageNet-S [39]			ImageNet-A [13]			ImageNet-R [12]		
			Acc_{leaf}	HCA	MTA									
CoOp	16		64.01	2.31	43.74	47.82	1.39	38.58	50.28	2.97	52.56	75.83	18.49	64.13
	16	✓	62.60	32.84	86.66	46.80	20.73	82.60	49.08	22.45	78.21	74.94	31.18	75.59
	1		56.43	1.51	38.27	41.38	1.11	33.61	45.92	1.76	47.54	69.84	11.74	55.31
	1	✓	60.16	22.95	84.38	44.75	13.88	80.64	48.95	20.52	76.95	74.26	27.46	76.48
MaPLe	16		(+3.73)	(+21.44)	(+46.11)	(+3.37)	(+12.77)	(+47.03)	(3.03)	(+18.76)	(+29.41)	(+4.42)	(+15.72)	(+21.17)
	16	✓	(-1.41)	(+30.53)	(+42.92)	(-1.02)	(+19.34)	(+44.02)	(-1.20)	(+19.48)	(+25.65)	(-0.89)	(+12.69)	(+11.40)
	1													
	1	✓												

These results show that ProTeCt robustifies the model for use in the coarse-granularity classification setting. The table also shows that ProTeCt maintains leaf accuracies comparable to those of the vanilla methods, even achieving slight gains for Cifar100 and SUN. Fig. 3 compares the **relative** gain of the HCA (Top row) and leaf accuracy (Bottom row) between the vanilla CoOp/MaPLe and their ProTeCt counterparts, for more few shot configurations. Under all settings, ProTeCt increases the HCA by more than 15% with comparable leaf accuracy to vanilla CoOp/MaPLe.

5.2 Improved Hierarchical Consistency Across Domains

Following the domain generalization setting of [50, 49, 15, 45], we investigate whether hierarchical consistency generalizes across datasets. More specifically, a CLIP model with ProTeCt prompts trained on ImageNet (source) is applied to 4 ImageNet variants (target) with domain shift: ImageNetv2 [34], ImageNet-Sketch [39], ImageNet-A [13] and ImageNet-R [12]. Table 3 summarizes the three metrics on these datasets for CoOp and MaPLe. Similarly to Table 2, ProTeCt enables significant gains in HCA and MTA over the baselines for all datasets. Note that, since ImageNet-A and ImageNet-R only contain 200 ImageNet subclasses, their hierarchy is different from that of ImageNet. These results demonstrate the flexibility and robustness of ProTeCt, even when transferring the model to a target domain whose class hierarchy is different from that of the source domain.

5.3 Ablation Study and Visualization

In this section, we discuss ablations of ProTeCt components and visualize the predictions of different models. More detailed ablations and visualizations can be found in the appendix.

Tree Dropout Rate β : Fig. 4 (a) plots Cifar100 Acc_{leaf} and HCA as a function of the drop-out rate β , for 16-shot CoOp + ProTeCt training ($\lambda = 1$). Larger values of β reduce the likelihood of sampling the leaf nodes of the tree, resulting in shorter trees and weaker regularization, in general. Hence, both leaf accuracy and HCA degrade for large β . On the other hand, always using the full tree ($\beta = 0$) also achieves sub-optimal results. The two metrics peak at $\beta = 0.1$ and $\beta = 0.2$, respectively, and $\beta = 0.1$ is selected for all our experiments.

NCL strength λ : Fig. 4(b) summarizes the Cifar100 performance of 1-shot classification with CoOp and $\beta = 0.1$, as a function of the hyperparameter λ that balances the two losses of (11). The introduction of NCL improves leaf accuracy/HCA from 64.8/32.9 ($\lambda = 0$) to 66.9/41 ($\lambda = 0.5$). We adopt $\lambda = 0.5$ for CIFAR100 and SUN. For ImageNet, $\lambda = 0.5$ and $\lambda = 1$ have comparable performance. See appendix for more discussion.

Architecture: Fig. 4 (c) shows that the gains observed for CoOp+ProTeCt with CLIP ViT B16 features in Fig. 3 also hold for ViT B32 features, highlighting the plug-and-play properties of ProTeCt.

Visualization: Fig. 5 shows examples from ImageNet (a,b), ImageNet-A (c) and ImageNet-R (d). While ProTeCt can correctly classify these examples at all hierarchy levels, vanilla prompt tuning fails at certain granularities. See more examples in appendix.

6 Related Work

Prompt Tuning for Vision-Language Models. Many large vision-language foundational models have been proposed in recent years [46, 9, 40]. Despite their promising zero-shot performance, several works [49, 50, 14, 15] show that their finetuning with a few examples from the target dataset can further improve performance. Unlike conventional finetuning methods that optimize the entire model, these methods are designed to (a) be parameter efficient and (b) maintain the general purpose

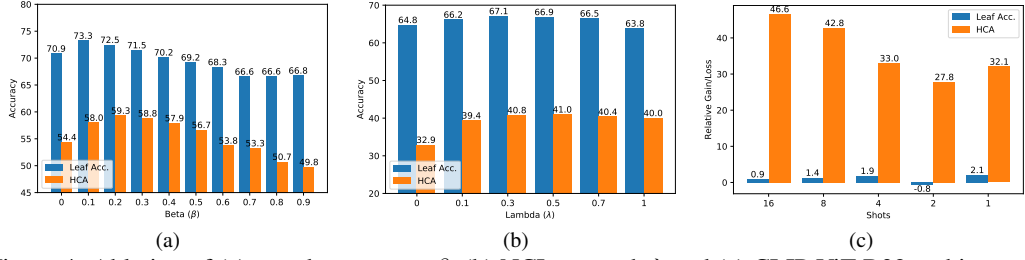


Figure 4: Ablation of (a) tree dropout rate β , (b) NCL strength λ and (c) CLIP ViT B32 architecture.



Figure 5: ProTeCt correctly predicts examples from ImageNet (a,b) and its variants (c,d) at all levels. [GT, Prediction] shows the **groundtruth** and **incorrect prediction** by vanilla prompt tuning.

feature representation of the foundational model. Several such tuning methods have been proposed for CLIP [33] (refer to section 2 for more details). Inspired by prompt tuning techniques from the language literature [20, 22, 24], CoOp [50] proposed to fine-tune CLIP on few-shot examples, by inserting learnable prompts at the CLIP text input. CoCoOp [49] further learns a meta-network to generate an image-conditioned prompt. The idea of connecting image and text prompts is also adopted by UPT [45] and MaPLe [15], where the former learns a unified transformer for generating an image and text prompt, and the latter learns a coupling function to generate image prompts from text prompts, inside the transformer layers. LASP [2] proposed a text-to-text cross-entropy loss to regularize the distribution shift when different prompts are used. R-Tuning [23] aims to address the open-set classification problem and proposes to introduce open words from WordNet to extend the prompt text. Unlike these works, we investigate the problem of open-granularity classification, where labels can be drawn from any level in a class taxonomy, and propose prompting techniques to improve hierarchical classification consistency. This is shown to be possible for several of the prior prompt-tuning methods, without degrading their leaf classification accuracy.

Hierarchical Classifiers. Hierarchical classification aims to predict labels at different levels of a class hierarchy. Early works [29, 48, 5, 35, 36, 7] date back to the era before deep learning and are not directly applicable to deep learning-based models. Several works [44, 11, 51, 25, 1, 16] propose hierarchical classifiers for CNN-based deep models. For example, [11, 51, 25] use additional convolutional modules to learn a hierarchical feature space. It is unclear whether these approaches can generalize to recent transformer-based models [8, 27, 26]. Furthermore, prior works [44, 11, 51, 25, 1, 42] finetune the entire model, which requires substantial data and is computationally inefficient. In this work, we study the problem of hierarchical consistency for foundational vision-language models (e.g., CLIP). While CLIP-based classifiers [33, 49, 50] have outstanding zero/few-shot performance, they produce inconsistent predictions for label sets of different granularity and have poor performance for open-granularity classification. We propose an efficient prompt tuning method to address this.

7 Conclusions

In this work, we propose ProTeCt for enhancing the hierarchical consistency of CLIP and existing prompt tuning methods. For a given dataset, a class hierarchy is built by assigning the dataset classes to leaf nodes and superclasses to internal nodes. A dynamic treecut loss, based on an efficient treecut sampler, is proposed to dynamically regularize labels of varying granularity, during prompt tuning. A node-centric loss is then proposed to encourage correct predictions at all hierarchy levels. Experiments show that ProTeCt enhances the hierarchical consistency of existing prompt tuning techniques and that hierarchical consistency transfers to unseen domains.

8 Acknowledgments

This work was partially funded by NSF awards IIS-1924937 and IIS-2041009, a gift from Amazon, a gift from Qualcomm, and NVIDIA GPU donations. We also acknowledge and thank the use of the Nautilus platform for some of the experiments discussed above.

References

- [1] Karim Ahmed, Mohammad Haris Baig, and Lorenzo Torresani. Network of experts for large-scale image categorization. In *European Conference on Computer Vision (ECCV)*, 2016.
- [2] Adrian Bulat and Georgios Tzimiropoulos. Lasp: Text-to-text optimization for language-aware soft prompting of vision&language models. In *The IEEE/CVF Conference on Computer Vision and Pattern Recognition*, 2023.
- [3] Ting Chen, Simon Kornblith, Mohammad Norouzi, and Geoffrey Hinton. A simple framework for contrastive learning of visual representations. In *Proceedings of the 37th International Conference on Machine Learning, ICML'20*. JMLR.org, 2020.
- [4] Xinlei Chen, Haoqi Fan, Ross B. Girshick, and Kaiming He. Improved baselines with momentum contrastive learning. *ArXiv*, abs/2003.04297, 2020.
- [5] Jia Deng, Nan Ding, Yangqing Jia, Andrea Frome, Kevin Murphy, Samy Bengio, Yuan Li, Hartmut Neven, and Hartwig Adam. Large-scale object classification using label relation graphs. In *European Conference on Computer Vision (ECCV)*, 2014.
- [6] Jia Deng, Wei Dong, Richard Socher, Li-Jia Li, Kai Li, and Li Fei-Fei. Imagenet: A large-scale hierarchical image database. In *2009 IEEE Conference on Computer Vision and Pattern Recognition*, pages 248–255, 2009.
- [7] Jia Deng, Jonathan Krause, Alexander C. Berg, and Li Fei-Fei. Hedging your bets: Optimizing accuracy-specificity trade-offs in large scale visual recognition. In *IEEE Conference on Computer Vision and Pattern Recognition (CVPR)*, 2012.
- [8] Alexey Dosovitskiy, Lucas Beyer, Alexander Kolesnikov, Dirk Weissenborn, Xiaohua Zhai, Thomas Unterthiner, Mostafa Dehghani, Matthias Minderer, Georg Heigold, Sylvain Gelly, Jakob Uszkoreit, and Neil Houlsby. An image is worth 16x16 words: Transformers for image recognition at scale. In *International Conference on Learning Representations*, 2021.
- [9] Yifan Du, Zikang Liu, Junyi Li, and Wayne Xin Zhao. A survey of vision-language pre-trained models. In *International Joint Conference on Artificial Intelligence*, 2022.
- [10] Christiane Fellbaum, editor. *WordNet: An Electronic Lexical Database*. Language, Speech, and Communication. MIT Press, Cambridge, MA, 1998.
- [11] Wonjoon Goo, Juyong Kim, Gunhee Kim, and Sung Ju Hwang. Taxonomy-regularized semantic deep convolutional neural networks. In *European Conference on Computer Vision (ECCV)*, 2016.
- [12] Dan Hendrycks, Steven Basart, Norman Mu, Saurav Kadavath, Frank Wang, Evan Dorundo, Rahul Desai, Tyler Lixuan Zhu, Samyak Parajuli, Mike Guo, Dawn Xiaodong Song, Jacob Steinhardt, and Justin Gilmer. The many faces of robustness: A critical analysis of out-of-distribution generalization. *2021 IEEE/CVF International Conference on Computer Vision (ICCV)*, pages 8320–8329, 2020.
- [13] Dan Hendrycks, Kevin Zhao, Steven Basart, Jacob Steinhardt, and Dawn Song. Natural adversarial examples. *CVPR*, 2021.
- [14] Menglin Jia, Luming Tang, Bor-Chun Chen, Claire Cardie, Serge Belongie, Bharath Hariharan, and Ser-Nam Lim. Visual prompt tuning. In *European Conference on Computer Vision (ECCV)*, 2022.
- [15] Muhammad Uzair khattak, Hanoona Rasheed, Muhammad Maaz, Salman Khan, and Fahad Shahbaz Khan. Maple: Multi-modal prompt learning. In *The IEEE/CVF Conference on Computer Vision and Pattern Recognition*, 2023.
- [16] Hyo Jin Kim and Jan-Michael Frahm. Hierarchy of alternating specialists for scene recognition. In *European Conference on Computer Vision (ECCV)*, 2018.
- [17] Jonathan Krause, Jia Deng, Michael Stark, and Li Fei-Fei. Collecting a large-scale dataset of fine-grained cars. 2013.
- [18] Alex Krizhevsky. Learning multiple layers of features from tiny images. 2009.
- [19] Kibok Lee, Kimin Lee, Kyle Min, Yuting Zhang, Jinwoo Shin, and Honglak Lee. Hierarchical novelty detection for visual object recognition. In *IEEE Conference on Computer Vision and Pattern Recognition (CVPR)*, 2018.
- [20] Brian Lester, Rami Al-Rfou, and Noah Constant. The power of scale for parameter-efficient prompt tuning. In *Proceedings of the 2021 Conference on Empirical Methods in Natural Language Processing*, pages 3045–3059, Online and Punta Cana, Dominican Republic, November 2021. Association for Computational Linguistics.
- [21] Fei-Fei Li, Marco Andreetto, Marc'Aurelio Ranzato, and Pietro Perona. Caltech 101, Apr 2022.

[22] Xiang Lisa Li and Percy Liang. Prefix-tuning: Optimizing continuous prompts for generation. In *Proceedings of the 59th Annual Meeting of the Association for Computational Linguistics and the 11th International Joint Conference on Natural Language Processing (Volume 1: Long Papers)*, pages 4582–4597, Online, August 2021. Association for Computational Linguistics.

[23] Ning Liao, Xiaopeng Zhang, Minglu Cao, Qi Tian, and Junchi Yan. R-tuning: Regularized prompt tuning in open-set scenarios. *ArXiv*, abs/2303.05122, 2023.

[24] Xiao Liu, Kaixuan Ji, Yicheng Fu, Weng Tam, Zhengxiao Du, Zhilin Yang, and Jie Tang. P-tuning: Prompt tuning can be comparable to fine-tuning across scales and tasks. In *Proceedings of the 60th Annual Meeting of the Association for Computational Linguistics (Volume 2: Short Papers)*, pages 61–68, Dublin, Ireland, May 2022. Association for Computational Linguistics.

[25] Yuntao Liu, Yong Dou, Ruochun Jin, and Peng Qiao. Visual tree convolutional neural network in image classification. In *International Conference on Pattern Recognition (ICPR)*, 2018.

[26] Ze Liu, Han Hu, Yutong Lin, Zhuliang Yao, Zhenda Xie, Yixuan Wei, Jia Ning, Yue Cao, Zheng Zhang, Li Dong, Furu Wei, and Baining Guo. Swin transformer v2: Scaling up capacity and resolution. In *International Conference on Computer Vision and Pattern Recognition (CVPR)*, 2022.

[27] Ze Liu, Yutong Lin, Yue Cao, Han Hu, Yixuan Wei, Zheng Zhang, Stephen Lin, and Baining Guo. Swin transformer: Hierarchical vision transformer using shifted windows. In *Proceedings of the IEEE/CVF International Conference on Computer Vision (ICCV)*, 2021.

[28] Timo Lüddecke and Alexander Ecker. Image segmentation using text and image prompts. In *Proceedings of the IEEE/CVF Conference on Computer Vision and Pattern Recognition (CVPR)*, pages 7086–7096, June 2022.

[29] Marcin Marszałek and Cordelia Schmid. Semantic hierarchies for visual object recognition. In *IEEE Conference on Computer Vision and Pattern Recognition (CVPR)*, 2007.

[30] Maria-Elena Nilsback and Andrew Zisserman. Automated flower classification over a large number of classes. In *2008 Sixth Indian Conference on Computer Vision, Graphics & Image Processing*, pages 722–729, 2008.

[31] Adam Paszke, Sam Gross, Francisco Massa, Adam Lerer, James Bradbury, Gregory Chanan, Trevor Killeen, Zeming Lin, Natalia Gimelshein, Luca Antiga, Alban Desmaison, Andreas Kopf, Edward Yang, Zachary DeVito, Martin Raison, Alykhan Tejani, Sasank Chilamkurthy, Benoit Steiner, Lu Fang, Junjie Bai, and Soumith Chintala. Pytorch: An imperative style, high-performance deep learning library. In H. Wallach, H. Larochelle, A. Beygelzimer, F. d'Alché-Buc, E. Fox, and R. Garnett, editors, *Advances in Neural Information Processing Systems 32*, pages 8024–8035. Curran Associates, Inc., 2019.

[32] Songyou Peng, Kyle Genova, Chiyu "Max" Jiang, Andrea Tagliasacchi, Marc Pollefeys, and Thomas Funkhouser. Openscene: 3d scene understanding with open vocabularies. In *CVPR*, 2023.

[33] Alec Radford, Jong Wook Kim, Chris Hallacy, Aditya Ramesh, Gabriel Goh, Sandhini Agarwal, Girish Sastry, Amanda Askell, Pamela Mishkin, Jack Clark, Gretchen Krueger, and Ilya Sutskever. Learning transferable visual models from natural language supervision. In *International Conference on Machine Learning*, 2021.

[34] Benjamin Recht, Rebecca Roelofs, Ludwig Schmidt, and Vaishaal Shankar. Do imagenet classifiers generalize to imagenet? In *International Conference on Machine Learning*, 2019.

[35] Ruslan Salakhutdinov, Antonio Torralba, and Josh Tenenbaum. Learning to share visual appearance for multiclass object detection. In *IEEE Conference on Computer Vision and Pattern Recognition (CVPR)*, 2011.

[36] Babak Shahbaba and Radford M. Neal. Improving classification when a class hierarchy is available using a hierarchy-based prior. *Bayesian Analysis*, 2(1):221–238, 2007.

[37] Kihyuk Sohn. Improved deep metric learning with multi-class n-pair loss objective. In *NIPS*, 2016.

[38] Aäron van den Oord, Yazhe Li, and Oriol Vinyals. Representation learning with contrastive predictive coding. *ArXiv*, abs/1807.03748, 2018.

[39] Haohan Wang, Songwei Ge, Zachary Lipton, and Eric P Xing. Learning robust global representations by penalizing local predictive power. In *Advances in Neural Information Processing Systems*, pages 10506–10518, 2019.

[40] Xiao Wang, Guangyao Chen, Guangwu Qian, Pengcheng Gao, Xiaoyong Wei, Yaowei Wang, Yonghong Tian, and Wen Gao. Large-scale multi-modal pre-trained models: A comprehensive survey. *ArXiv*, abs/2302.10035, 2023.

[41] Zhaoqing Wang, Yu Lu, Qiang Li, Xunqiang Tao, Yandong Guo, Mingming Gong, and Tongliang Liu. Cris: Clip-driven referring image segmentation. In *Proceedings of the IEEE/CVF conference on computer vision and pattern recognition*, 2022.

- [42] Tz-Ying Wu, Pedro Morgado, Pei Wang, Chih-Hui Ho, and Nuno Vasconcelos. Solving long-tailed recognition with deep realistic taxonomic classifier. In *European Conference on Computer Vision (ECCV)*, 2020.
- [43] Jianxiong Xiao, James Hays, Krista A. Ehinger, Aude Oliva, and Antonio Torralba. Sun database: Large-scale scene recognition from abbey to zoo. In *2010 IEEE Computer Society Conference on Computer Vision and Pattern Recognition*, pages 3485–3492, 2010.
- [44] Zhicheng Yan, Hao Zhang, Robinson Piramuthu, Vignesh Jagadeesh, Dennis DeCoste, Wei Di, and Yizhou Yu. Hd-cnn: Hierarchical deep convolutional neural networks for large scale visual recognition. In *International Conference on Computer Vision (ICCV)*, 2015.
- [45] Yuhang Zang, Wei Li, Kaiyang Zhou, Chen Huang, and Chen Change Loy. Unified vision and language prompt learning. *ArXiv*, abs/2210.07225, 2022.
- [46] Jingyi Zhang, Jiaxing Huang, Sheng Jin, and Shijian Lu. Vision-language models for vision tasks: A survey. *ArXiv*, abs/2304.00685, 2023.
- [47] Renrui Zhang, Ziyu Guo, Wei Zhang, Kunchang Li, Xupeng Miao, Bin Cui, Yu Qiao, Peng Gao, and Hongsheng Li. Pointclip: Point cloud understanding by clip. *arXiv preprint arXiv:2112.02413*, 2021.
- [48] Bin Zhao, Li Fei-Fei, and Eric P. Xing. Large-scale category structure aware image categorization. In *Advances in Neural Information Processing Systems (NIPS)*, 2011.
- [49] Kaiyang Zhou, Jingkang Yang, Chen Change Loy, and Ziwei Liu. Conditional prompt learning for vision-language models. In *IEEE/CVF Conference on Computer Vision and Pattern Recognition (CVPR)*, 2022.
- [50] Kaiyang Zhou, Jingkang Yang, Chen Change Loy, and Ziwei Liu. Learning to prompt for vision-language models. *International Journal of Computer Vision (IJCV)*, 2022.
- [51] Xinqi Zhu and Michael Bain. B-cnn: Branch convolutional neural network for hierarchical classification. *CoRR*, abs/1709.09890, 2017.

Appendix

The appendix is organized as follows. Section A provides more training details for ProTeCt. Section B shows more examples for explaining the implementation of treecut sampler. Section C, Section D, and Section E shows the complete results conducted on Cifar100, Sun and ImageNet, respectively. Section E further shows the complete domain generalization results by applying the model trained on ImageNet to its 4 variants in a zero-shot fashion. Ablations of different ProTeCt components are shown in Section F and more visualizations of incorrect predictions from existing prompt tuning methods are illustrated in Section G.

A Additional Training Details

In addition to the training details provided in the main paper, we list the url links that are used for training and evaluating ProTeCt. For CoOp and CoCoOp baselines, we adopt the code from <https://github.com/KaiyangZhou/CoOp>. For MaPLe, we adopt the code from <https://github.com/muzairkhattak/multimodal-prompt-learning>.

B Additional Examples for Treecut Sampler

In this section, we provide more detailed examples of the proposed Treecut sampler (i.e. Algorithm 1). Given the class hierarchy \mathcal{T} on the left of Figure B1, three possible treecuts can be sampled by \mathcal{T} , i.e., $\mathcal{Y}_{\mathcal{T}_c} = \{n_1, n_6\}$ (see Figure B1), $\mathcal{Y}_{\mathcal{T}_c} = \{n_2, n_3, n_6\}$ (see Figure B2), and $\mathcal{Y}_{\mathcal{T}_c} = \{n_3, n_4, n_5, n_6\}$ (see Figure B3), depending on the sampled values p_n at each internal node $n \in \mathcal{N}^{int} = \{n_0, n_1, n_2\}$. Note that p_{n_0} is always set to 1 to ensure that the tree is not entirely pruned. As described in the paper, we use a dependency matrix \mathbf{D} to correct \mathbf{p} as $\tilde{\mathbf{p}}$, which is aligned with the dependency relationship among the internal nodes. For example, in the example shown in Figure B1, $p_{n_2} = 1$ is corrected as $\tilde{p}_{n_2} = 0$, since n_2 depends on n_1 and $p_{n_1} = 0$. A mask \mathbf{b} , flagging the unavailable labels, is then computed according to the values of $\tilde{\mathbf{p}}$. More specifically, the corresponding row in $\text{min}(\mathbf{B}, 0)$ is fetched when $\tilde{p}_n = 1$, and that in $\tilde{\mathbf{B}}$ is used when $\tilde{p}_n = 0$, for each internal node $n \in \mathcal{N}^{int}$. These masks are accumulated into the final mask \mathbf{b} , as shown on the right of each figure, where entries of 0 indicate the available labels for the sampled label set. For example, in Figure B2, the sampled label set contains $\{n_2, n_3, n_6\}$, because b_2, b_3 and b_6 are 0s.

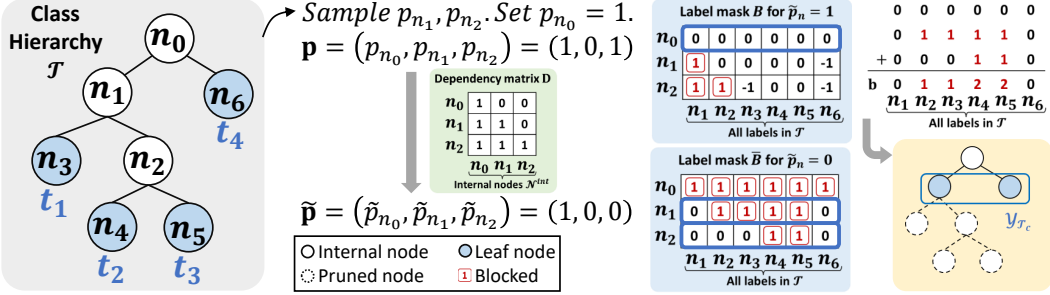


Figure B1: Treecut example of $\mathcal{Y}_{\mathcal{T}_c} = \{n_1, n_6\}$.

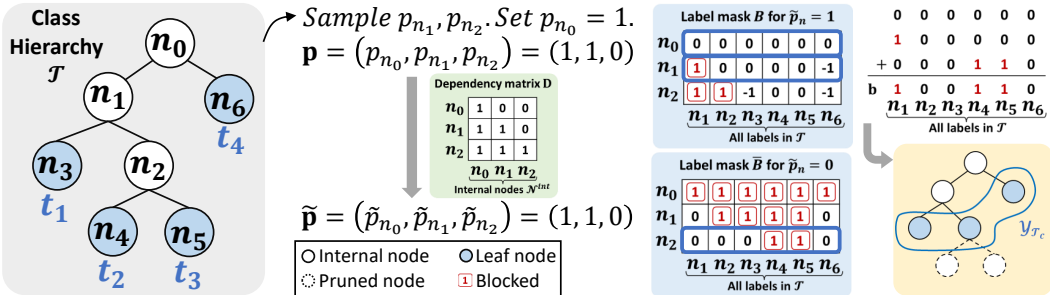


Figure B2: Treecut example of $\mathcal{Y}_{\mathcal{T}_c} = \{n_2, n_3, n_6\}$.

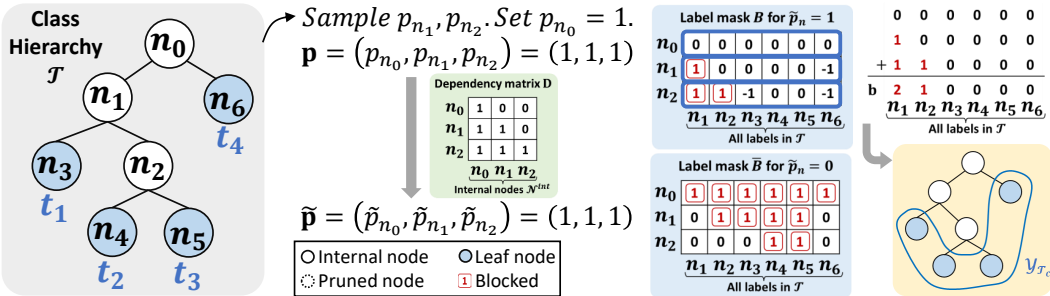


Figure B3: Treecut example of $\mathcal{Y}_{\mathcal{T}_c} = \{n_3, n_4, n_5, n_6\}$.

C Complete Table of Cifar100 Experiments

In this section, we report the complete experiment results conducted on Cifar100. Table C1, Table C2 and Table C3 shows the results of vanilla CoOp and its results after adding ProTeCt. The CLIP features from ViT B16, ViT B32 and ViT L14 are considered in Table C1, Table C2 and Table C3, respectively. While it is known that CLIP ViT L14 has a more powerful representation than ViT B32 and ViT B16 (also reflected on the leaf accuracy between three tables), all of them perform equally poor in terms of HCA ($10.04/4.95/11.14$ for 16-shot CoOp using CLIP B16/B32/L14 feature). This shows that simply using a stronger CLIP feature does not address the problem of hierarchical classification and does not improve hierarchical consistency. Furthermore, Table C1 contains the result of ProTeCt without using the treecut sampler ($\beta = 0$; Block 2 and Block 3) and without using NCL loss of (7) ($\lambda = 0$; Block 4) under multiple low-shot settings. For example, when 16-shot is considered, adding both NCL loss and treecut sampler ($\lambda = 0.5$ and $\beta = 0.1$) gives the result of 56.85 for HCA. Removing the tree dropout ($\lambda = 0.5$ and $\beta = 0$) yields 51.99 and removing the NCL loss ($\lambda = 0$ and $\beta = 0.1$) yields 47.97. This shows that both the NCL loss and the treecut sampler are important and lead to a significant gain over vanilla CoOp (HCA=10.04). Table C4 shows similar results when adding ProTeCt on MaPLe. Furthermore, we sampled T treecuts for each dropout rate $\beta = \{0.1, 0.3, 0.5, 0.7, 0.9\}$, where $T = 5$ and $T = 20$, resulting in 25 and 100 treecuts, respectively. Table C5 demonstrates ProTeCt can improve the MTA metric for both CoOp and MaPLe for both 25 and 100 randomly sampled treecuts.

Table C1: Performance of few-shot CoOp on Cifar100 under ViT B16. Ablations cover both NCL strengths λ and tree dropout rate β .

Method	Encoder	K-shot	w/ ProTeCt	λ	β	Leaf Acc.	HCA
CoOp	ViT B16	16		N/A	N/A	72.88 ± 0.62	10.04 ± 1.11
CoOp	ViT B16	8		N/A	N/A	70.84 ± 0.85	6.03 ± 0.64
CoOp	ViT B16	4		N/A	N/A	69.47 ± 0.90	6.15 ± 1.04
CoOp	ViT B16	2		N/A	N/A	68.17 ± 0.57	4.19 ± 0.81
CoOp	ViT B16	1		N/A	N/A	65.03 ± 0.56	7.81 ± 0.14
CoOp	ViT B16	16	✓	0.5	0	72.08 ± 0.38	51.99 ± 0.24
CoOp	ViT B16	8	✓	0.5	0	68.94 ± 0.52	49.01 ± 0.54
CoOp	ViT B16	4	✓	0.5	0	66.38 ± 1.18	45.24 ± 0.93
CoOp	ViT B16	2	✓	0.5	0	63.96 ± 0.57	42.78 ± 1.49
CoOp	ViT B16	1	✓	0.5	0	62.01 ± 0.80	34.90 ± 1.08
CoOp	ViT B16	16	✓	1	0	70.86 ± 0.59	54.39 ± 0.68
CoOp	ViT B16	8	✓	1	0	68.76 ± 0.90	52.14 ± 0.32
CoOp	ViT B16	4	✓	1	0	66.92 ± 0.20	47.63 ± 0.54
CoOp	ViT B16	2	✓	1	0	64.87 ± 1.28	40.74 ± 0.87
CoOp	ViT B16	1	✓	1	0	62.57 ± 0.06	38.97 ± 1.29
CoOp	ViT B16	16	✓	0	0.1	72.81 ± 0.31	47.97 ± 0.70
CoOp	ViT B16	8	✓	0	0.1	70.94 ± 0.18	48.53 ± 0.02
CoOp	ViT B16	4	✓	0	0.1	69.10 ± 0.92	45.20 ± 0.25
CoOp	ViT B16	2	✓	0	0.1	68.85 ± 0.11	42.28 ± 1.57
CoOp	ViT B16	1	✓	0	0.1	64.77 ± 1.37	32.93 ± 0.42
CoOp	ViT B16	16	✓	0.5	0.1	72.94 ± 0.83	56.85 ± 1.60
CoOp	ViT B16	8	✓	0.5	0.1	71.10 ± 1.06	52.27 ± 0.62
CoOp	ViT B16	4	✓	0.5	0.1	69.46 ± 0.58	48.71 ± 0.13
CoOp	ViT B16	2	✓	0.5	0.1	68.63 ± 0.67	46.03 ± 0.24
CoOp	ViT B16	1	✓	0.5	0.1	66.88 ± 0.21	41.01 ± 1.18
CoOp	ViT B16	16	✓	1	0.1	73.26 ± 0.66	58.01 ± 0.43
CoOp	ViT B16	8	✓	1	0.1	70.10 ± 0.08	52.81 ± 0.05
CoOp	ViT B16	4	✓	1	0.1	68.41 ± 0.50	49.59 ± 0.89
CoOp	ViT B16	2	✓	1	0.1	67.73 ± 1.25	45.27 ± 0.28
CoOp	ViT B16	1	✓	1	0.1	63.84 ± 1.51	40.05 ± 1.48

Table C2: Performance of few-shot CoOp on Cifar100 under ViT B32. Ablations cover different NCL strengths λ .

Method	Encoder	K-shot	w/ ProTeCt	λ	β	Leaf Acc.	HCA
CoOp	ViT B32	16		N/A	N/A	68.13 \pm 0.19	4.95 \pm 0.61
CoOp	ViT B32	8		N/A	N/A	65.52 \pm 0.15	5.82 \pm 0.29
CoOp	ViT B32	4		N/A	N/A	63.42 \pm 1.40	8.56 \pm 0.72
CoOp	ViT B32	2		N/A	N/A	63.65 \pm 0.60	10.25 \pm 0.88
CoOp	ViT B32	1		N/A	N/A	59.53 \pm 0.60	3.43 \pm 0.86
CoOp	ViT B32	16	✓	0	0.1	68.42 \pm 0.91	47.79 \pm 0.54
CoOp	ViT B32	8	✓	0	0.1	66.39 \pm 0.48	44.47 \pm 0.98
CoOp	ViT B32	4	✓	0	0.1	64.73 \pm 0.17	31.72 \pm 0.33
CoOp	ViT B32	2	✓	0	0.1	64.55 \pm 0.44	30.78 \pm 0.66
CoOp	ViT B32	1	✓	0	0.1	60.91 \pm 0.42	34.64 \pm 0.55
CoOp	ViT B32	8	✓	0.5	0.1	68.87 \pm 1.09	51.55 \pm 0.65
CoOp	ViT B32	4	✓	0.5	0.1	66.85 \pm 0.32	48.39 \pm 1.35
CoOp	ViT B32	2	✓	0.5	0.1	65.41 \pm 0.74	41.63 \pm 0.39
CoOp	ViT B32	16	✓	0.5	0.1	62.86 \pm 0.81	38.13 \pm 0.61
CoOp	ViT B32	1	✓	0.5	0.1	61.59 \pm 0.80	35.65 \pm 0.19
CoOp	ViT B32	16	✓	1	0.1	68.93 \pm 0.22	51.67 \pm 0.58
CoOp	ViT B32	8	✓	1	0.1	65.54 \pm 0.54	48.36 \pm 0.63
CoOp	ViT B32	4	✓	1	0.1	64.28 \pm 0.07	42.78 \pm 1.04
CoOp	ViT B32	2	✓	1	0.1	61.68 \pm 0.67	40.53 \pm 0.42
CoOp	ViT B32	1	✓	1	0.1	58.98 \pm 0.88	36.59 \pm 0.76

Table C3: Performance of few-shot CoOp on Cifar100 under both ViT L14. Ablations cover different NCL strengths λ .

Method	Encoder	K-shot	w/ ProTeCt	λ	β	Leaf Acc.	HCA
CoOp	ViT L14	16		N/A	N/A	79.98 \pm 0.97	11.14 \pm 0.47
CoOp	ViT L14	8		N/A	N/A	79.37 \pm 0.90	6.91 \pm 0.67
CoOp	ViT L14	4		N/A	N/A	77.34 \pm 0.78	7.78 \pm 0.82
CoOp	ViT L14	2		N/A	N/A	76.63 \pm 0.65	5.21 \pm 0.87
CoOp	ViT L14	1		N/A	N/A	73.26 \pm 0.95	4.87 \pm 0.15
CoOp	ViT L14	16	✓	0	0.1	81.17 \pm 0.34	63.40 \pm 0.30
CoOp	ViT L14	8	✓	0	0.1	80.00 \pm 0.98	62.11 \pm 0.81
CoOp	ViT L14	4	✓	0	0.1	79.05 \pm 0.68	57.19 \pm 0.26
CoOp	ViT L14	2	✓	0	0.1	78.53 \pm 0.69	40.59 \pm 0.68
CoOp	ViT L14	1	✓	0	0.1	76.48 \pm 0.52	45.11 \pm 0.68
CoOp	ViT L14	8	✓	0.5	0.1	80.95 \pm 0.38	68.92 \pm 0.77
CoOp	ViT L14	4	✓	0.5	0.1	79.87 \pm 0.11	64.05 \pm 0.57
CoOp	ViT L14	2	✓	0.5	0.1	79.18 \pm 0.51	51.88 \pm 0.45
CoOp	ViT L14	16	✓	0.5	0.1	76.76 \pm 0.24	51.96 \pm 0.06
CoOp	ViT L14	1	✓	0.5	0.1	73.89 \pm 0.62	50.31 \pm 1.02
CoOp	ViT L14	16	✓	1	0.1	80.45 \pm 0.90	70.15 \pm 0.98
CoOp	ViT L14	8	✓	1	0.1	79.25 \pm 0.93	65.75 \pm 0.69
CoOp	ViT L14	4	✓	1	0.1	78.37 \pm 0.13	47.30 \pm 0.20
CoOp	ViT L14	2	✓	1	0.1	75.21 \pm 0.33	54.78 \pm 0.66
CoOp	ViT L14	1	✓	1	0.1	74.93 \pm 0.15	52.08 \pm 1.04

Table C4: Performance of few-shot MaPLE on Cifar100. Ablations cover different NCL strengths λ .

Method	Encoder	K-shot	w/ ProTeCt	λ	β	Leaf Acc.	HCA
MaPLE	ViT B16	16		N/A	N/A	75.01 \pm 0.37	17.54 \pm 0.83
MaPLE	ViT B16	8		N/A	N/A	73.93 \pm 0.46	9.44 \pm 1.13
MaPLE	ViT B16	4		N/A	N/A	72.68 \pm 0.47	20.29 \pm 1.07
MaPLE	ViT B16	2		N/A	N/A	71.37 \pm 1.39	12.15 \pm 0.25
MaPLE	ViT B16	1		N/A	N/A	68.75 \pm 0.96	4.65 \pm 1.52
MaPLE	ViT B16	16	✓	0	0.1	75.82 \pm 0.10	58.63 \pm 0.43
MaPLE	ViT B16	8	✓	0	0.1	74.29 \pm 0.91	57.31 \pm 0.79
MaPLE	ViT B16	4	✓	0	0.1	72.92 \pm 0.42	54.12 \pm 1.56
MaPLE	ViT B16	2	✓	0	0.1	71.09 \pm 1.35	47.78 \pm 0.64
MaPLE	ViT B16	1	✓	0	0.1	68.32 \pm 0.20	39.43 \pm 0.25
MaPLE	ViT B16	16	✓	0.5	0.1	75.34 \pm 0.39	61.15 \pm 0.53
MaPLE	ViT B16	8	✓	0.5	0.1	74.30 \pm 0.29	60.24 \pm 0.82
MaPLE	ViT B16	4	✓	0.5	0.1	71.35 \pm 0.61	56.03 \pm 0.35
MaPLE	ViT B16	2	✓	0.5	0.1	70.24 \pm 1.01	52.56 \pm 0.48
MaPLE	ViT B16	1	✓	0.5	0.1	69.33 \pm 0.81	48.10 \pm 0.26
MaPLE	ViT B16	16	✓	1	0.1	76.30 \pm 0.56	62.04 \pm 0.97
MaPLE	ViT B16	8	✓	1	0.1	73.60 \pm 0.69	61.20 \pm 0.77
MaPLE	ViT B16	4	✓	1	0.1	72.06 \pm 0.34	56.51 \pm 1.24
MaPLE	ViT B16	2	✓	1	0.1	69.95 \pm 1.30	53.53 \pm 0.67
MaPLE	ViT B16	1	✓	1	0.1	70.44 \pm 0.10	46.94 \pm 0.85

Table C5: Performance of MTA for both few-shot CoOp and MaPLe on Cifar100. 25 ($T = 5$) and 100 ($T = 20$) treecuts are sampled for MTA evaluation.

Method	Encoder	K-shot	w/ ProTeCt	λ	β	MTA (25)	MTA (100)
CoOp	ViT B32	16		N/A	N/A	52.33	54.58
CoOp	ViT B32	8		N/A	N/A	46.09	47.20
CoOp	ViT B32	4		N/A	N/A	53.35	54.30
CoOp	ViT B32	2		N/A	N/A	53.13	53.81
CoOp	ViT B32	1		N/A	N/A	38.80	40.16
CoOp	ViT B32	16	✓	0.5	0.1	86.26	85.73
CoOp	ViT B32	8	✓	0.5	0.1	85.05	84.57
CoOp	ViT B32	4	✓	0.5	0.1	81.01	80.61
CoOp	ViT B32	2	✓	0.5	0.1	79.95	79.98
CoOp	ViT B32	1	✓	0.5	0.1	78.08	76.95
CoOp	ViT B16	16		N/A	N/A	50.64	51.14
CoOp	ViT B16	8		N/A	N/A	47.95	50.41
CoOp	ViT B16	4		N/A	N/A	43.77	46.29
CoOp	ViT B16	2		N/A	N/A	40.81	42.95
CoOp	ViT B16	1		N/A	N/A	41.78	44.17
CoOp	ViT B16	16	✓	0.5	0.1	87.69	87.30
CoOp	ViT B16	8	✓	0.5	0.1	86.28	86.01
CoOp	ViT B16	4	✓	0.5	0.1	84.52	83.79
CoOp	ViT B16	2	✓	0.5	0.1	83.49	83.18
CoOp	ViT B16	1	✓	0.5	0.1	81.64	81.01
CoOp	ViT L14	16		N/A	N/A	58.81	60.89
CoOp	ViT L14	8		N/A	N/A	40.49	43.20
CoOp	ViT L14	4		N/A	N/A	44.71	47.39
CoOp	ViT L14	2		N/A	N/A	39.44	43.22
CoOp	ViT L14	1		N/A	N/A	52.32	54.90
CoOp	ViT L14	16	✓	0.5	0.1	90.83	90.48
CoOp	ViT L14	8	✓	0.5	0.1	89.39	89.16
CoOp	ViT L14	4	✓	0.5	0.1	84.48	84.79
CoOp	ViT L14	2	✓	0.5	0.1	85.57	85.29
CoOp	ViT L14	1	✓	0.5	0.1	83.65	83.52
MaPLe	ViT B16	16		N/A	N/A	52.21	50.82
MaPLe	ViT B16	8		N/A	N/A	58.56	61.48
MaPLe	ViT B16	4		N/A	N/A	66.14	67.06
MaPLe	ViT B16	2		N/A	N/A	55.98	57.59
MaPLe	ViT B16	1		N/A	N/A	50.60	54.99
MaPLe	ViT B16	16	✓	0.5	0.1	88.04	88.33
MaPLe	ViT B16	8	✓	0.5	0.1	87.65	88.13
MaPLe	ViT B16	4	✓	0.5	0.1	86.72	87.04
MaPLe	ViT B16	2	✓	0.5	0.1	85.03	85.39
MaPLe	ViT B16	1	✓	0.5	0.1	83.36	83.78

D Complete Table of SUN Experiments

In this section, we report the complete experiment result conducted on SUN. Table D1 and Table D2 show the results of vanilla CoOp and MaPLe, and their results after adding ProTeCt. When comparing the HCA results of the vanilla prompt tuning with that of Cifar100 and ImageNet, the HCA result on SUN is much higher and the gap between HCA and Acc_{leaf} is much smaller. This is due to the shallow hierarchy of SUN dataset, indicating SUN is a much simpler dataset for hierarchical classification. However, we still see that ProTeCt achieves consistent improvement over the vanilla prompt tuning methods. Table D3 further compares the MTA result of vanilla CoOp and MaPLe, and their ProTeCt counterpart.

Table D1: Performance of few-shot CoOp on SUN. Ablations cover different NCL strengths λ .

Method	Encoder	K-shot	w/ ProTeCt	λ	β	Leaf Acc.	HCA
CoOp	ViT B16	16		N/A	N/A	73.82 \pm 0.12	38.28 \pm 0.46
CoOp	ViT B16	8		N/A	N/A	71.77 \pm 0.67	33.95 \pm 0.08
CoOp	ViT B16	4		N/A	N/A	69.31 \pm 0.51	30.51 \pm 0.71
CoOp	ViT B16	2		N/A	N/A	66.34 \pm 0.33	36.85 \pm 0.67
CoOp	ViT B16	1		N/A	N/A	63.65 \pm 1.42	33.36 \pm 0.21
CoOp	ViT B16	16	✓	0	0.1	74.95 \pm 0.69	60.95 \pm 0.91
CoOp	ViT B16	8	✓	0	0.1	72.31 \pm 0.18	57.61 \pm 1.31
CoOp	ViT B16	4	✓	0	0.1	69.53 \pm 0.77	54.79 \pm 0.12
CoOp	ViT B16	2	✓	0	0.1	67.01 \pm 1.10	50.78 \pm 0.03
CoOp	ViT B16	1	✓	0	0.1	64.45 \pm 0.96	47.75 \pm 0.11
CoOp	ViT B16	8	✓	0.5	0.1	74.59 \pm 0.41	62.94 \pm 0.15
CoOp	ViT B16	4	✓	0.5	0.1	71.53 \pm 0.67	58.17 \pm 0.33
CoOp	ViT B16	2	✓	0.5	0.1	69.80 \pm 0.98	56.85 \pm 0.41
CoOp	ViT B16	16	✓	0.5	0.1	67.29 \pm 1.32	51.82 \pm 1.20
CoOp	ViT B16	1	✓	0.5	0.1	63.79 \pm 1.16	49.62 \pm 1.40
CoOp	ViT B16	16	✓	1	0.1	74.31 \pm 0.23	62.96 \pm 0.61
CoOp	ViT B16	8	✓	1	0.1	71.27 \pm 0.42	58.74 \pm 0.98
CoOp	ViT B16	4	✓	1	0.1	68.81 \pm 0.71	55.90 \pm 0.09
CoOp	ViT B16	2	✓	1	0.1	67.66 \pm 0.51	50.94 \pm 1.31
CoOp	ViT B16	1	✓	1	0.1	63.95 \pm 1.19	50.99 \pm 1.21

Table D2: Performance of few-shot MaPLe on SUN. Ablations cover different NCL strengths λ .

Method	Encoder	K-shot	w/ ProTeCt	λ	β	Leaf Acc.	HCA
MaPLe	ViT B16	16		N/A	N/A	71.86 \pm 0.11	33.25 \pm 1.31
MaPLe	ViT B16	8		N/A	N/A	68.96 \pm 0.51	29.63 \pm 0.19
MaPLe	ViT B16	4		N/A	N/A	67.27 \pm 0.45	25.97 \pm 0.53
MaPLe	ViT B16	2		N/A	N/A	65.33 \pm 1.21	29.79 \pm 0.13
MaPLe	ViT B16	1		N/A	N/A	63.98 \pm 0.99	25.15 \pm 0.76
MaPLe	ViT B16	16	✓	0	0.1	72.89 \pm 0.77	56.52 \pm 0.88
MaPLe	ViT B16	8	✓	0	0.1	71.24 \pm 0.76	55.49 \pm 1.05
MaPLe	ViT B16	4	✓	0	0.1	69.24 \pm 0.41	51.88 \pm 1.22
MaPLe	ViT B16	2	✓	0	0.1	66.98 \pm 0.44	51.60 \pm 0.55
MaPLe	ViT B16	1	✓	0	0.1	63.80 \pm 1.51	47.93 \pm 0.31
MaPLe	ViT B16	16	✓	0.5	0.1	72.17 \pm 1.20	59.71 \pm 0.04
MaPLe	ViT B16	8	✓	0.5	0.1	71.04 \pm 0.09	57.78 \pm 1.22
MaPLe	ViT B16	4	✓	0.5	0.1	68.64 \pm 0.61	54.86 \pm 1.08
MaPLe	ViT B16	2	✓	0.5	0.1	66.37 \pm 0.62	53.13 \pm 0.39
MaPLe	ViT B16	1	✓	0.5	0.1	64.29 \pm 1.23	50.45 \pm 0.40
MaPLe	ViT B16	16	✓	1	0.1	71.03 \pm 0.99	59.92 \pm 0.06
MaPLe	ViT B16	8	✓	1	0.1	69.66 \pm 0.16	57.60 \pm 0.81
MaPLe	ViT B16	4	✓	1	0.1	66.96 \pm 0.31	53.61 \pm 0.55
MaPLe	ViT B16	2	✓	1	0.1	66.74 \pm 0.36	53.54 \pm 0.76
MaPLe	ViT B16	1	✓	1	0.1	63.46 \pm 0.14	50.49 \pm 1.01

Table D3: Performance of MTA for both few-shot CoOp and MaPLE on Sun.

Method	Encoder	K-shot	w/ ProTeCt	λ	β	MTA
CoOp	ViT B16	16		N/A	N/A	52.99
CoOp	ViT B16	8		N/A	N/A	55.24
CoOp	ViT B16	4		N/A	N/A	49.48
CoOp	ViT B16	2		N/A	N/A	51.94
CoOp	ViT B16	1		N/A	N/A	51.20
CoOp	ViT B16	16	✓	0.5	0.1	83.51
CoOp	ViT B16	8	✓	0.5	0.1	81.34
CoOp	ViT B16	4	✓	0.5	0.1	80.30
CoOp	ViT B16	2	✓	0.5	0.1	76.59
CoOp	ViT B16	1	✓	0.5	0.1	76.25
MaPLE	ViT B16	16		N/A	N/A	54.29
MaPLE	ViT B16	8		N/A	N/A	53.24
MaPLE	ViT B16	4		N/A	N/A	55.79
MaPLE	ViT B16	2		N/A	N/A	51.30
MaPLE	ViT B16	1		N/A	N/A	50.31
MaPLE	ViT B16	16	✓	0.5	0.1	82.27
MaPLE	ViT B16	8	✓	0.5	0.1	80.71
MaPLE	ViT B16	4	✓	0.5	0.1	79.10
MaPLE	ViT B16	2	✓	0.5	0.1	77.55
MaPLE	ViT B16	1	✓	0.5	0.1	76.73

E Complete Table of ImageNet Experiments

In this section, we report the complete experiment result conducted on ImageNet. Table E1 first show the performance of CLIP and CoCoOp as a complement of Table 1 in the main paper. Note that none of the CLIP features (e.g. ViT B32, ViT B16, RN50, RN101) nor existing prompt tuning methods help the HCA metric. Table E2 and Table E3 show the results of vanilla CoOp and MaPLE, and their results after adding ProTeCt. Table E4 further compares the MTA result of vanilla CoOp and MaPLE, and their ProTeCt counterpart. Clearly, adding ProTeCt boosts both HCA and MTA. Furthermore, we apply the model trained on ImageNet to its four variants. Table E5, Table E6, Table E7 and Table E8 report the domain generalization results on ImageNetV2, ImageNet-sketch, ImageNet-A and ImageNet-R datasets for Acc_{leaf} , HCA and MTA. All four tables show that ProTeCt can not only improves the hierarchical consistency on the seen dataset, but also unseen datasets from other image domains.

Table E1: Performance of zero-shot CLIP and 16-shot CoCoOp on ImageNet.

Method	Encoder	K-shot	w/ ProTeCt	λ	β	Leaf Acc.	HCA
CLIP	ViT-B32	0		N/A	N/A	63.31	4.29
CLIP	ViT-B16	0		N/A	N/A	68.36	3.32
CLIP	RN50	0		N/A	N/A	59.81	4.16
CLIP	RN101	0		N/A	N/A	62.30	2.03
CoCoOp	ViT-B16	16		N/A	N/A	71.20 ± 0.13	2.92 ± 1.23

Table E2: Performance of few-shot CoOp on ImageNet. Ablations cover different NCL strengths λ .

Method	Encoder	K-shot	w/ ProTeCt	λ	β	Leaf Acc.	HCA
CoOp	ViT B16	16		N/A	N/A	71.23 \pm 0.67	2.99 \pm 1.04
CoOp	ViT B16	8		N/A	N/A	69.40 \pm 0.52	3.00 \pm 0.58
CoOp	ViT B16	4		N/A	N/A	68.06 \pm 0.42	2.95 \pm 0.62
CoOp	ViT B16	2		N/A	N/A	65.46 \pm 0.77	1.56 \pm 0.17
CoOp	ViT B16	1		N/A	N/A	63.67 \pm 0.85	1.59 \pm 0.43
CoOp	ViT B16	16	✓	0	0.1	70.47 \pm 0.22	27.81 \pm 0.71
CoOp	ViT B16	8	✓	0	0.1	70.03 \pm 0.14	26.17 \pm 0.52
CoOp	ViT B16	4	✓	0	0.1	69.32 \pm 0.11	21.99 \pm 0.10
CoOp	ViT B16	2	✓	0	0.1	68.09 \pm 0.23	20.92 \pm 1.02
CoOp	ViT B16	1	✓	0	0.1	67.26 \pm 0.65	18.69 \pm 1.12
CoOp	ViT B16	8	✓	0.5	0.1	70.27 \pm 0.36	34.63 \pm 0.33
CoOp	ViT B16	4	✓	0.5	0.1	69.65 \pm 0.41	31.84 \pm 0.35
CoOp	ViT B16	2	✓	0.5	0.1	68.09 \pm 0.16	27.05 \pm 0.27
CoOp	ViT B16	16	✓	0.5	0.1	67.24 \pm 0.24	26.09 \pm 0.53
CoOp	ViT B16	1	✓	0.5	0.1	66.69 \pm 0.15	23.79 \pm 0.15
CoOp	ViT B16	16	✓	1	0.1	69.92 \pm 0.21	37.74 \pm 0.12
CoOp	ViT B16	8	✓	1	0.1	69.34 \pm 0.17	34.66 \pm 0.55
CoOp	ViT B16	4	✓	1	0.1	68.06 \pm 0.44	30.87 \pm 0.32
CoOp	ViT B16	2	✓	1	0.1	67.12 \pm 0.35	26.34 \pm 1.1
CoOp	ViT B16	1	✓	1	0.1	66.11 \pm 0.50	25.79 \pm 0.06

Table E3: Performance of few-shot MaPLe on ImageNet. Ablations cover different NCL strengths λ .

Method	Encoder	K-shot	w/ ProTeCt	λ	β	Leaf Acc.	HCA
MaPLe	ViT B16	16		N/A	N/A	70.70 \pm 0.11	4.15 \pm 1.05
MaPLe	ViT B16	8		N/A	N/A	70.44 \pm 0.06	4.32 \pm 0.90
MaPLe	ViT B16	4		N/A	N/A	70.20 \pm 0.06	2.95 \pm 0.87
MaPLe	ViT B16	2		N/A	N/A	69.74 \pm 0.25	4.27 \pm 1.32
MaPLe	ViT B16	1		N/A	N/A	68.91 \pm 0.13	2.97 \pm 1.08
MaPLe	ViT B16	16	✓	0	0.1	70.08 \pm 0.26	23.38 \pm 1.43
MaPLe	ViT B16	8	✓	0	0.1	69.00 \pm 0.26	21.71 \pm 0.64
MaPLe	ViT B16	4	✓	0	0.1	68.50 \pm 0.41	19.03 \pm 0.21
MaPLe	ViT B16	2	✓	0	0.1	67.45 \pm 0.32	17.54 \pm 0.52
MaPLe	ViT B16	1	✓	0	0.1	67.03 \pm 0.11	16.54 \pm 0.32
MaPLe	ViT B16	16	✓	0.5	0.1	69.59 \pm 0.25	27.74 \pm 1.31
MaPLe	ViT B16	8	✓	0.5	0.1	69.06 \pm 0.49	25.25 \pm 0.52
MaPLe	ViT B16	4	✓	0.5	0.1	68.13 \pm 0.01	25.25 \pm 0.12
MaPLe	ViT B16	2	✓	0.5	0.1	67.45 \pm 0.43	20.14 \pm 1.07
MaPLe	ViT B16	1	✓	0.5	0.1	66.80 \pm 0.26	20.62 \pm 0.65
MaPLe	ViT B16	16	✓	1	0.1	69.52 \pm 0.71	31.24 \pm 1.02
MaPLe	ViT B16	8	✓	1	0.1	68.48 \pm 0.06	26.92 \pm 0.42
MaPLe	ViT B16	4	✓	1	0.1	68.59 \pm 0.17	26.28 \pm 0.31
MaPLe	ViT B16	2	✓	1	0.1	67.12 \pm 0.11	22.96 \pm 0.05
MaPLe	ViT B16	1	✓	1	0.1	66.16 \pm 0.88	20.44 \pm 0.77

Table E4: Performance of MTA for both few-shot CoOp and MaPLe on ImageNet.

Method	Encoder	K-shot	w/ ProTeCt	λ	β	MTA
CoOp	ViT B16	16		N/A	N/A	46.98
CoOp	ViT B16	8		N/A	N/A	46.04
CoOp	ViT B16	4		N/A	N/A	42.57
CoOp	ViT B16	2		N/A	N/A	44.89
CoOp	ViT B16	1		N/A	N/A	40.52
CoOp	ViT B16	16	✓	0.5	0.1	88.61
CoOp	ViT B16	8	✓	0.5	0.1	87.86
CoOp	ViT B16	4	✓	0.5	0.1	87.37
CoOp	ViT B16	2	✓	0.5	0.1	86.14
CoOp	ViT B16	1	✓	0.5	0.1	86.14
MaPLe	ViT B16	16		N/A	N/A	48.29
MaPLe	ViT B16	8		N/A	N/A	45.84
MaPLe	ViT B16	4		N/A	N/A	51.84
MaPLe	ViT B16	2		N/A	N/A	48.17
MaPLe	ViT B16	1		N/A	N/A	48.16
MaPLe	ViT B16	16	✓	0.5	0.1	87.87
MaPLe	ViT B16	8	✓	0.5	0.1	87.26
MaPLe	ViT B16	4	✓	0.5	0.1	86.85
MaPLe	ViT B16	2	✓	0.5	0.1	85.93
MaPLe	ViT B16	1	✓	0.5	0.1	85.18

Table E5: Domain generalization on ImageNetv2 dataset using CoOp and MaPLe.

Method	Encoder	K-shot	w/ ProTeCt	λ	β	Leaf Acc.	HCA	MTA
CoOp	ViT B16	16		N/A	N/A	64.01	2.31	43.74
CoOp	ViT B16	8		N/A	N/A	62.20	2.62	43.30
CoOp	ViT B16	4		N/A	N/A	61.51	2.48	40.68
CoOp	ViT B16	2		N/A	N/A	58.68	1.35	42.84
CoOp	ViT B16	1		N/A	N/A	56.43	1.51	38.27
CoOp	ViT B16	16	✓	1	0.1	62.60	32.84	86.66
CoOp	ViT B16	8	✓	1	0.1	62.15	30.65	85.84
CoOp	ViT B16	4	✓	1	0.1	61.24	26.85	85.52
CoOp	ViT B16	2	✓	1	0.1	60.42	23.22	84.38
CoOp	ViT B16	1	✓	1	0.1	60.16	22.95	84.38
MaPLe	ViT B16	16		N/A	N/A	64.15	1.97	45.93
MaPLe	ViT B16	8		N/A	N/A	62.76	1.99	43.98
MaPLe	ViT B16	4		N/A	N/A	63.45	2.51	49.41
MaPLe	ViT B16	2		N/A	N/A	61.75	2.81	45.92
MaPLe	ViT B16	1		N/A	N/A	61.78	2.18	45.50
MaPLe	ViT B16	16	✓	1	0.1	62.77	27.86	86.14
MaPLe	ViT B16	8	✓	1	0.1	61.42	23.45	85.51
MaPLe	ViT B16	4	✓	1	0.1	61.89	22.92	85.17
MaPLe	ViT B16	2	✓	1	0.1	60.43	20.10	84.23
MaPLe	ViT B16	1	✓	1	0.1	59.14	17.89	83.27

Table E6: Domain generalization on ImageNet-sketch dataset using CoOp and MaPLe.

Method	Encoder	K-shot	w/ ProTeCt	λ	β	Leaf Acc.	HCA	MTA
CoOp	ViT B16	16		N/A	N/A	47.82	1.39	38.58
CoOp	ViT B16	8		N/A	N/A	45.93	2.10	42.56
CoOp	ViT B16	4		N/A	N/A	44.60	1.41	36.52
CoOp	ViT B16	2		N/A	N/A	42.17	0.96	36.01
CoOp	ViT B16	1		N/A	N/A	41.38	1.11	33.61
CoOp	ViT B16	16	✓	1	0.1	46.80	20.73	82.60
CoOp	ViT B16	8	✓	1	0.1	46.91	19.71	82.11
CoOp	ViT B16	4	✓	1	0.1	46.53	17.69	82.07
CoOp	ViT B16	2	✓	1	0.1	45.40	15.49	80.82
CoOp	ViT B16	1	✓	1	0.1	44.75	13.88	80.64
MaPLe	ViT B16	16		N/A	N/A	48.97	1.58	43.37
MaPLe	ViT B16	8		N/A	N/A	47.55	1.66	45.26
MaPLe	ViT B16	4		N/A	N/A	48.20	2.45	53.31
MaPLe	ViT B16	2		N/A	N/A	46.86	1.01	42.55
MaPLe	ViT B16	1		N/A	N/A	46.79	1.70	45.26
MaPLe	ViT B16	16	✓	1	0.1	47.47	17.77	82.52
MaPLe	ViT B16	8	✓	1	0.1	46.60	15.31	82.04
MaPLe	ViT B16	4	✓	1	0.1	47.23	14.95	81.67
MaPLe	ViT B16	2	✓	1	0.1	45.95	13.32	80.87
MaPLe	ViT B16	1	✓	1	0.1	44.92	11.24	79.94

Table E7: Domain generalization on ImageNet-A dataset using CoOp and MaPLe.

Method	Encoder	K-shot	w/ ProTeCt	λ	β	Leaf Acc.	HCA	MTA
CoOp	ViT B16	16		N/A	N/A	50.28	2.97	52.56
CoOp	ViT B16	8		N/A	N/A	48.08	4.19	45.05
CoOp	ViT B16	4		N/A	N/A	48.43	2.97	41.20
CoOp	ViT B16	2		N/A	N/A	46.56	1.95	52.47
CoOp	ViT B16	1		N/A	N/A	45.92	1.76	47.54
CoOp	ViT B16	16	✓	1	0.1	49.08	22.45	78.21
CoOp	ViT B16	8	✓	1	0.1	49.29	24.00	79.47
CoOp	ViT B16	4	✓	1	0.1	48.39	18.11	76.95
CoOp	ViT B16	2	✓	1	0.1	48.81	20.00	78.11
CoOp	ViT B16	1	✓	1	0.1	48.95	20.52	76.95
MaPLe	ViT B16	16		N/A	N/A	50.61	2.31	54.88
MaPLe	ViT B16	8		N/A	N/A	48.41	5.31	55.97
MaPLe	ViT B16	4		N/A	N/A	50.23	4.95	57.07
MaPLe	ViT B16	2		N/A	N/A	48.49	9.80	59.90
MaPLe	ViT B16	1		N/A	N/A	47.55	3.52	55.48
MaPLe	ViT B16	16	✓	1	0.1	47.41	19.75	77.46
MaPLe	ViT B16	8	✓	1	0.1	46.15	16.49	75.88
MaPLe	ViT B16	4	✓	1	0.1	47.35	17.39	77.64
MaPLe	ViT B16	2	✓	1	0.1	49.15	16.23	77.71
MaPLe	ViT B16	1	✓	1	0.1	47.15	16.03	76.81

Table E8: Domain generalization on ImageNet-R dataset using CoOp and MaPLE.

Method	Encoder	K-shot	w/ ProTeCt	λ	β	Leaf Acc.	HCA	MTA
CoOp	ViT B16	16		N/A	N/A	75.83	18.49	64.13
CoOp	ViT B16	8		N/A	N/A	74.79	5.91	49.56
CoOp	ViT B16	4		N/A	N/A	73.99	14.85	61.40
CoOp	ViT B16	2		N/A	N/A	70.94	16.32	56.67
CoOp	ViT B16	1		N/A	N/A	69.84	11.74	55.31
CoOp	ViT B16	16	✓	1	0.1	74.94	31.18	75.59
CoOp	ViT B16	8	✓	1	0.1	75.51	37.96	81.11
CoOp	ViT B16	4	✓	1	0.1	74.23	29.69	75.54
CoOp	ViT B16	2	✓	1	0.1	74.86	28.67	78.17
CoOp	ViT B16	1	✓	1	0.1	74.26	27.46	76.48
MaPLE	ViT B16	16		N/A	N/A	76.61	20.67	63.06
MaPLE	ViT B16	8		N/A	N/A	76.48	18.92	67.30
MaPLE	ViT B16	4		N/A	N/A	76.83	21.06	64.30
MaPLE	ViT B16	2		N/A	N/A	75.85	19.84	60.86
MaPLE	ViT B16	1		N/A	N/A	74.55	18.85	62.48
MaPLE	ViT B16	16	✓	1	0.1	75.70	32.58	77.99
MaPLE	ViT B16	8	✓	1	0.1	75.98	30.97	77.57
MaPLE	ViT B16	4	✓	1	0.1	76.31	29.28	78.52
MaPLE	ViT B16	2	✓	1	0.1	75.01	23.94	72.73
MaPLE	ViT B16	1	✓	1	0.1	74.60	25.20	75.72

F Complete Ablation Results

This section complements Figure 4(a) and 4(b) in the main paper with the error bar. Table F1 and Table F2 show how the NCL strength λ and tree dropout rates β affect the Acc_{leaf} and HCA. Please refer to Section 5.3 of the main paper for more discussion.

Table F1: Ablation of different NCL strength λ on Cifar100 using CoOp 1 shot setting.

Method	Encoder	K-shot	w/ ProTeCt	λ	β	Leaf Acc.	HCA
CoOp	ViT B16	1	✓	0	0.1	64.77 ± 1.37	32.93 ± 0.42
CoOp	ViT B16	1	✓	0.1	0.1	66.18 ± 0.51	39.41 ± 0.78
CoOp	ViT B16	1	✓	0.3	0.1	67.13 ± 0.66	40.82 ± 0.33
CoOp	ViT B16	1	✓	0.5	0.1	66.88 ± 0.21	41.01 ± 1.18
CoOp	ViT B16	1	✓	0.7	0.1	66.50 ± 0.71	40.39 ± 0.37
CoOp	ViT B16	1	✓	1	0.1	63.84 ± 1.51	40.05 ± 1.48

Table F2: Ablation of different tree dropout rates β on Cifar100 using CoOp 16 shot setting.

Method	Encoder	K-shot	w/ ProTeCt	λ	β	Leaf Acc.	HCA
CoOp	ViT B16	16	✓	1	0	70.86 ± 0.59	54.39 ± 0.68
CoOp	ViT B16	16	✓	1	0.1	73.26 ± 0.66	58.01 ± 0.43
CoOp	ViT B16	16	✓	1	0.2	72.48 ± 0.57	59.32 ± 0.21
CoOp	ViT B16	16	✓	1	0.3	71.49 ± 0.36	58.82 ± 0.12
CoOp	ViT B16	16	✓	1	0.4	70.15 ± 0.75	57.93 ± 0.50
CoOp	ViT B16	16	✓	1	0.5	69.22 ± 0.32	56.66 ± 0.41
CoOp	ViT B16	16	✓	1	0.6	68.35 ± 0.78	53.75 ± 0.85
CoOp	ViT B16	16	✓	1	0.7	66.58 ± 0.45	53.27 ± 0.42
CoOp	ViT B16	16	✓	1	0.8	66.62 ± 0.38	50.74 ± 1.05
CoOp	ViT B16	16	✓	1	0.9	66.77 ± 0.38	49.76 ± 1.02

G Visualizations

This section illustrates some misclassified examples of prior prompt tuning methods in ImageNet and its variants (i.e. ImageNetv2, ImageNet-S, ImageNet-A, ImageNet-R). The misclassification can occur in both coarse or fine-grained levels of the hierarchy. Note that ProTeCt can successfully classify all the illustrated examples at **every** hierarchy level in the examples shown in Figure G1-G5, where [GT, Prediction] shows the **groundtruth** and **incorrect prediction** by vanilla prompt tuning.



Figure G1: ImageNet visual examples: (a): [Leopard, Person], (b): [School bus, Scoreboard], (c):[Restaurant, Organism], (d): [Chihuahua, Person], (e): [Mop, Bath towel].

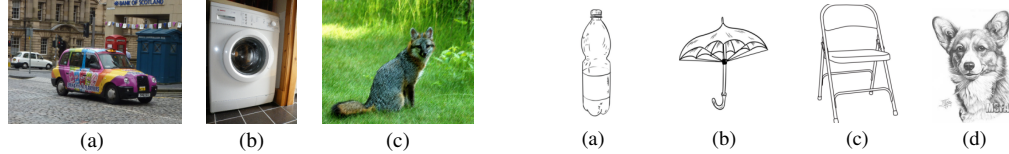


Figure G2: ImageNetv2 visual examples: (a): [Taxicab, Teddy bear], (b): [Washing machine, Bath towel], (c):[Grey fox, Marsupial].

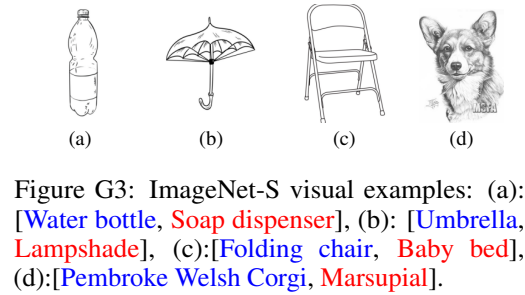


Figure G3: ImageNet-S visual examples: (a): [Water bottle, Soap dispenser], (b): [Umbrella, Lampshade], (c):[Folding chair, Baby bed], (d):[Pembroke Welsh Corgi, Marsupial].

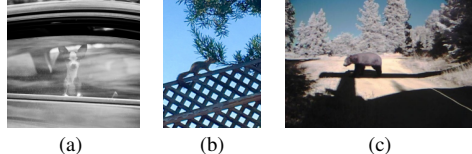


Figure G4: ImageNet-A visual examples: (a): [Chihuahua, Cottontail rabbit], (b): [Fox squirrel, Bird], (c):[American black bear, Koala].

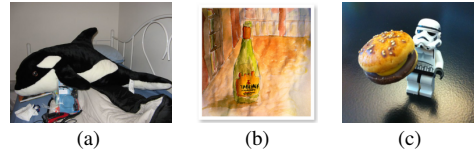


Figure G5: ImageNet-R visual examples: (a): [Killer whale, Person], (b): [Wine bottle, Fruit], (c):[Cheeseburger, Ice cream].